

Decays of B meson to two charmed mesons

Run-Hui Li^{1,2}, Cai-Dian Lü^{1,4}, A.I. Sanda³, and Xiao-Xia Wang¹

¹ *Institute of High Energy Physics, P.O. Box 918(4), Beijing 100049, People's Republic of China*

² *School of Physics, Shandong University, Jinan 250100, People's Republic of China*

³ *Faculty of Technology, Kanagawa University, Yokohama, Kanagawa 221, Japan*

⁴ *Theoretical Physics Center for Science Facilities, Beijing 100049, People's Republic of China*

The factorization theorem in decays of $B_{(s)}$ mesons to two charmed mesons (both pseudoscalar and vector) can be proved in the leading order in m_D/m_B and Λ_{QCD}/m_D expansion. Working in the perturbative QCD approach, we find that the factorizable emission diagrams are dominant. Most of branching ratios we compute agree with the experimental data well, which means that the factorization theorem seems to be reliable in predicting branching ratios for these decays. In the decays of a B meson to two vector charmed mesons, the transverse polarization states contribute 40% – 50% both in the processes with an external W emission and in the pure annihilation decays. This is in agreement with the present experimental data. We also calculate the CP asymmetry parameters. The results show that the direct CP asymmetries are very small. Thus observation of any large direct CP asymmetry will be a signal for new physics. The mixing induced CP asymmetry in the neutral modes is large. This is also in agreement with the current experimental measurements. They can give a cross check of the $\sin 2\beta$ measurement from other channels.

PACS numbers: 13.25.Hw, 12.38.Bx

I. INTRODUCTION

The hadronic decays of B meson are important for particle physics since they provide constraints of the standard model Cabibbo-Kobayashi-Maskawa (CKM) matrix, a test of the QCD factorization, information on the decay mechanism, and the final state interaction. The CP asymmetries, in which some of the hadronic uncertainties are canceled in their theoretical predictions, play an important role in the investigations of B physics. For the decays with a single D meson in the final states, only tree operators contribute, and thus no CP asymmetry appears in the standard model [1]. However, for decays with double-charm final states, there are penguin operator contributions as well as tree operator contributions. Thus the direct CP asymmetry may be present. Recently, the Belle Collaboration reported a large direct CP violation in $B^0 \rightarrow D^+ D^-$ decay [2], while BaBar reported a small one, with a different sign even [3]. What is more, large direct CP asymmetries have not been observed in other $B^0 \rightarrow D^{*+} D^{*-}$ decays [4] either, which have the same flavor structures as $B^0 \rightarrow D^+ D^-$ at the quark level. Intrigued by these experimental results, many investigations on the decays of B to double-charm states have been carried out [5–8].

The theoretical study of hadronic B decays has achieved great success in recent years. Among them, the perturbative QCD approach (PQCD) is based on k_T factorization [9]. By keeping the transverse momentum of quarks, the end point singularity in the collinear factorization has been eliminated. Since transverse momentum introduces another

energy scale, double logarithm appears in the QCD radiative corrections. The renormalization group equation is used to resum the double logarithm, which results in the Sudakov factor. This factor effectively suppresses the endpoint contribution of the distribution amplitude of mesons in the small transverse momentum region, which makes the perturbative calculation reliable. Phenomenologically, the PQCD approach successfully predict the following: (1)the direct CP asymmetry in B decays [10], (2)the pure annihilation type B decays [11] (3) the strong final state interaction phase and color suppressed decay amplitude in the $B \rightarrow D\pi$ decays [1].

In charmless two-body B decays, the final state mesons can be considered as massless therefore both of the final state mesons are on the light cone. The collinear factorization can be easily proved in the heavy quark limit. For the decays with a single heavy D meson in the final states, one can still prove factorization [12] in the leading order of the $r = m_D/m_B$ expansion. For the decays with double-charm quarks in the final states, such as $B \rightarrow J/\psi K, \chi_c K$, it is believed that the factorization fails. However the decays with double D mesons in the final states are different. The reason is that the expansion parameter $m_D/m_B \sim 0.36$ could be considered small, $m_{J/\psi}/m_B \sim 0.6$ is not. In other words, the J/ψ (χ_c) are soft particles in B decays; while the $D_{(s)}^{(*)}$ meson is collinear in the $B \rightarrow D_{(s)}^{(*)}D_{(s)}^{(*)}$ decays. The momentum of the $D_{(s)}^{(*)}$ meson in the latter decays is $|\vec{p}| \simeq \frac{1}{2}m_B(1 - 2r^2)$, which is still nearly half of the B meson mass. The decays of B to double-charm states can be investigated in the PQCD approach in the leading order of $r = m_D/m_B$ and Λ_{QCD}/m_D expansion. All of the annihilation type diagrams contain end-point singularity, which are quite different from the spectatorlike diagrams which are dominated by the form factors. It is very difficult to deal with in the collinear factorization. The PQCD base on k_T factorization is almost the only approach that can give quantitative calculations of annihilation type decays.

This paper is organized as follows. In Sec. II, we list the formalism, including the Hamiltonian, the wave functions of the mesons, the factorization formulae of the Feynman diagrams for $B \rightarrow PP$ decay mode, and the analytic expressions for the decay amplitudes. In Sec. III, the numerical results of the physical observables and discussions of the results are given. Sec. IV is a brief summary. The common PQCD functions, scales, and the factorization formulae of the Feynman diagrams for $B \rightarrow PV, B \rightarrow VP$, and $B \rightarrow VV$ modes are all put into the appendices for simplicity.

II. ANALYTIC EXPRESSIONS

In hadronic B decays there are several typical energy scales, and expansions with respect to the ratios of the scales are usually carried out. The physics with a scale higher than the W boson mass are electroweak interactions, which can be calculated perturbatively. The physics between the W boson mass and b quark mass obtain QCD corrections. This correction is included in the Wilson coefficients of the four-quark operators in the effective Hamiltonian. The physics below the b quark mass is more complicated. We have to utilize the factorization theorem to factorize the nonperturbative contributions out, so that the hard part can be calculated perturbatively. In the PQCD approach, we utilize the k_T factorization [9], where the transverse momenta of the quarks in the mesons are kept to eliminate the end-point singularity. Because of the new transverse momentum scale introduction, double logarithms appear in the calculation. We resum these logarithms to give a Sudakov factor, which effectively suppresses the end-point

region contribution. Thus the end-point singularity in the usual collinear factorization disappears. This makes the perturbative calculation reliable and consistent. For decays with D meson in the final states, another scale m_D is introduced. The factorization is proved in the leading order of the m_D/m_B expansion [12], therefore, as it is done in the computation of $B \rightarrow DM$ and $B \rightarrow \bar{D}M$ amplitudes[13], we will work in the leading order m_D/m_B expansion. For each of the diagrams in the following, we keep the contributions in the leading order of m_D/m_B . For example, in the B meson to two vector mesons decays, the leading order contributions of some transversely polarized amplitudes are proportional to r^2 ($r = m_D/m_B$). Then we will keep the r^2 terms in these diagrams. While in other cases, the terms of r^2 are neglected because the leading order is lower than 2. Finally the amplitude for $B \rightarrow M_2M_3$ (M_2 and M_3 stand for two mesons) decay within PQCD approach is decomposed as

$$\mathcal{M} = \int d^4k_1 d^4k_2 d^4k_3 \Phi_B(k_1, t) T_H(k_1, k_2, k_3, t) \Phi_{M_2}(k_2, t) \Phi_{M_3}(k_3, t) e^{S(k_i, t)}, \quad (1)$$

where k_i ($i = 1, 2, 3$) are the momenta of the quarks in mesons which are defined explicitly in Eq.(10). T_H is the hard part that is perturbatively calculable. Φ_B and Φ_{M_i} ($i = 2, 3$) are the hadronic meson wave functions that are treated as nonperturbative inputs. The Sudakov factors $e^{S(k_i, t)}$ ($i = 1, 2, 3$) are from the resummation of double logarithms .

A. Notations and conventions

The Hamiltonian referred to in this paper is given by [14]:

$$\begin{aligned} \mathcal{H}_{\text{eff}} = & \frac{G_F}{\sqrt{2}} \left\{ \sum_{q=u,c} V_{qb} V_{qD}^* [C_1(\mu) O_1^q(\mu) + C_2(\mu) O_2^q(\mu)] \right. \\ & \left. - V_{tb} V_{tD}^* \left[\sum_{i=3}^{10} C_i(\mu) O_i(\mu) \right] \right\} + \text{H.c.}, \end{aligned} \quad (2)$$

where $V_{qb(D)}$ and $V_{tb(D)}$ with $D = d, s$ are CKM matrix elements. Functions O_i ($i = 1, \dots, 10$) are local four-quark operators :

- current–current (tree) operators

$$O_1^q = (\bar{q}_\alpha b_\beta)_{V-A} (\bar{D}_\beta q_\alpha)_{V-A}, \quad O_2^q = (\bar{q}_\alpha b_\alpha)_{V-A} (\bar{D}_\beta q_\beta)_{V-A}, \quad (3)$$

- QCD penguin operators

$$O_3 = (\bar{D}_\alpha b_\alpha)_{V-A} \sum_{q'} (\bar{q}'_\beta q'_\beta)_{V-A}, \quad O_4 = (\bar{D}_\beta b_\alpha)_{V-A} \sum_{q'} (\bar{q}'_\alpha q'_\beta)_{V-A}, \quad (4)$$

$$O_5 = (\bar{D}_\alpha b_\alpha)_{V-A} \sum_{q'} (\bar{q}'_\beta q'_\beta)_{V+A}, \quad O_6 = (\bar{D}_\beta b_\alpha)_{V-A} \sum_{q'} (\bar{q}'_\alpha q'_\beta)_{V+A}, \quad (5)$$

- electro-weak penguin operators

$$O_7 = \frac{3}{2} (\bar{D}_\alpha b_\alpha)_{V-A} \sum_{q'} e_{q'} (\bar{q}'_\beta q'_\beta)_{V+A}, \quad O_8 = \frac{3}{2} (\bar{D}_\beta b_\alpha)_{V-A} \sum_{q'} e_{q'} (\bar{q}'_\alpha q'_\beta)_{V+A}, \quad (6)$$

$$O_9 = \frac{3}{2} (\bar{D}_\alpha b_\alpha)_{V-A} \sum_{q'} e_{q'} (\bar{q}'_\beta q'_\beta)_{V-A}, \quad O_{10} = \frac{3}{2} (\bar{D}_\beta b_\alpha)_{V-A} \sum_{q'} e_{q'} (\bar{q}'_\alpha q'_\beta)_{V-A}, \quad (7)$$

where α and β are color indices and q' are the active quarks at the scale m_b , i.e. $q' = (u, d, s, c, b)$. The left-handed current is defined as $(\bar{q}'_\alpha q'_\beta)_{V-A} = \bar{q}'_\alpha \gamma_\nu (1 - \gamma_5) q'_\beta$ and the right-handed current is $(\bar{q}'_\alpha q'_\beta)_{V+A} = \bar{q}'_\alpha \gamma_\nu (1 + \gamma_5) q'_\beta$. The combinations a_i of Wilson coefficients are defined as usual [15]:

$$\begin{aligned} a_1 &= C_2 + C_1/3, & a_2 &= C_1 + C_2/3, & a_3 &= C_3 + C_4/3, & a_4 &= C_4 + C_3/3, & a_5 &= C_5 + C_6/3, \\ a_6 &= C_6 + C_5/3, & a_7 &= C_7 + C_8/3, & a_8 &= C_8 + C_7/3, & a_9 &= C_9 + C_{10}/3, & a_{10} &= C_{10} + C_9/3. \end{aligned} \quad (8)$$

We work in the light-cone coordinate, in which a vector V^μ is defined as $(\frac{V^0+V^3}{\sqrt{2}}, \frac{V^0-V^3}{\sqrt{2}}, V^1, V^2)$. We use M_2 to denote the charmed meson with a c quark and M_3 to denote the meson with a \bar{c} quark. In this paper we work in the rest frame of B meson and define the direction in which M_2 moves as the positive direction of z -axis. Therefore the momenta of $B_{(s)}$ meson and two charmed mesons are defined in the light-cone coordinate as

$$p_B = \frac{m_B}{\sqrt{2}}(1, 1, \mathbf{0}_\perp), \quad p_2 = \frac{m_B}{\sqrt{2}}(1 - r_3^2, r_2^2, \mathbf{0}_\perp), \quad p_3 = \frac{m_B}{\sqrt{2}}(r_3^2, 1 - r_2^2, \mathbf{0}_\perp), \quad (9)$$

where $r_i = m_i/m_B$ ($i = 2, 3$) and $\mathbf{0}_\perp$ are zero two-component vectors. m_2 and m_3 are the masses of the two charmed mesons. One can find that our definitions of the momentums violate the on shell conditions. In the following calculations we will keep the contributions of each diagram to the leading power of r_i ($i = 2, 3$). One will find that all the terms with a power of r_i higher than 2 are dropped. At this accuracy level, the on-shell conditions can be satisfied. We use k_1 , k_2 , and k_3 to denote the momenta carried by the light quarks in $B_{(s)}$ meson and two charmed mesons. They are defined by

$$k_1 = (0, \frac{m_B}{\sqrt{2}}x_1, \mathbf{k}_{1\perp}), \quad k_2 = (\frac{m_B}{\sqrt{2}}(1 - r_3^2)x_2, 0, \mathbf{k}_{2\perp}), \quad k_3 = (0, \frac{m_B}{\sqrt{2}}(1 - r_2^2)x_3, \mathbf{k}_{3\perp}), \quad (10)$$

with x_1 , x_2 and x_3 as the momentum fractions.

B. Wave functions of $B_{(s)}$ mesons

The $B_{(s)}$ meson wave functions are decomposed into the following Lorentz structures:

$$\begin{aligned} & \int \frac{d^4 z}{(2\pi)^4} e^{ik_1 \cdot z} \langle 0 | \bar{b}_\alpha(0) d_\beta(z) | B_{(s)}(P_1) \rangle \\ &= \frac{i}{\sqrt{2N_c}} \left\{ (\not{P}_1 + m_{B_{(s)}}) \gamma_5 [\phi_{B_{(s)}}(k_1) - \frac{\not{h} - \not{k}}{\sqrt{2}} \bar{\phi}_{B_{(s)}}(k_1)] \right\}_{\beta\alpha}. \end{aligned} \quad (11)$$

Here, $\phi_{B_{(s)}}(k_1)$ and $\bar{\phi}_{B_{(s)}}(k_1)$ are the corresponding leading twist distribution amplitudes, and numerically $\bar{\phi}_{B_{(s)}}(k_1)$ gives small contributions [16], so we neglect it. The expression for $\Phi_{B_{(s)}}$ becomes

$$\Phi_{B_{(s)}} = \frac{i}{\sqrt{2N_c}} (\not{P}_1 + m_{B_{(s)}}) \gamma_5 \phi_{B_{(s)}}(k_1). \quad (12)$$

For the distribution amplitude in the b -space, we adopt the model function

$$\phi_{B_{(s)}}(x, b) = N_{B_{(s)}} x^2 (1-x)^2 \exp \left[-\frac{1}{2} \left(\frac{xm_{B_{(s)}}}{\omega_b} \right)^2 - \frac{\omega_b^2 b^2}{2} \right], \quad (13)$$

where b is the conjugate space coordinate of $\mathbf{k}_{1\perp}$. $N_{B(s)}$ is the normalization constant, which is determined by the normalization condition

$$\int_0^1 dx \phi_{B(s)}(x, b=0) = \frac{f_{B(s)}}{2\sqrt{2N_c}}. \quad (14)$$

The B^\pm and B_d^0 decays are studied intensively in PQCD approach[9]. With the rich experimental data the $\omega_b = 0.40$ GeV is determined for B meson. For B_s meson, we will follow the authors in Ref. [28] and adopt the value $\omega_{b_s} = (0.50 \pm 0.05)$ GeV.

C. Wave function of $D^{(*)}/\bar{D}^{(*)}$ meson

In the heavy quark limit, the two-particle light-cone distribution amplitudes of $D^{(*)}/\bar{D}^{(*)}$ meson are defined as[17]

$$\begin{aligned} \langle D(P_2) | q_\alpha(z) \bar{c}_\beta(0) | 0 \rangle &= \frac{i}{\sqrt{2N_c}} \int_0^1 dx e^{ixP_2 \cdot z} [\gamma_5 (\not{P}_2 + m_D) \phi_D(x, b)]_{\alpha\beta} \\ \langle D^*(P_2) | q_\alpha(z) \bar{c}_\beta(0) | 0 \rangle &= -\frac{1}{\sqrt{2N_c}} \int_0^1 dx e^{ixP_2 \cdot z} [\not{\epsilon}_L (\not{P}_2 + m_{D^*}) \phi_{D^*}^L(x, b) + \not{\epsilon}_T (\not{P}_2 + m_{D^*}) \phi_{D^*}^T(x, b)]_{\alpha\beta} \end{aligned} \quad (15)$$

with

$$\int_0^1 dx \phi_D(x, 0) = \frac{f_D}{2\sqrt{2N_c}}, \quad \int_0^1 dx \phi_{D^*}^L(x, 0) = \frac{f_{D^*}}{2\sqrt{2N_c}}, \quad \int_0^1 dx \phi_{D^*}^T(x, 0) = \frac{f_{D^*}^T}{2\sqrt{2N_c}}, \quad (16)$$

as the normalization conditions. In the heavy quark limit we have

$$f_{D^*}^T - f_{D^*} \frac{m_c + m_d}{M_{D^*}} \sim f_{D^*} - f_{D^*}^T \frac{m_c + m_d}{M_{D^*}} \sim O(\bar{\Lambda}/M_{D^*}). \quad (17)$$

Thus we will use $f_{D^*}^T = f_{D^*}$ in our calculation. The model for the distribution amplitude for D meson that we used in this paper is

$$\phi_D(x, b) = \frac{1}{2\sqrt{2N_c}} f_D 6x(1-x)[1 + C_D(1-2x)] \exp\left[\frac{-\omega^2 b^2}{2}\right], \quad (18)$$

which has been tested in the $B \rightarrow D^{(*)}M$ and $B \rightarrow \bar{D}^{(*)}M$ decays [13]. The masses of $D_{(s)}^{(*)}$ meson that we use are [18]

$$\begin{aligned} m_D &= 1.869 \text{ GeV}, & m_{D_s^-} &= 1.968 \text{ GeV}, \\ m_{D^*} &= 2.010 \text{ GeV}, & m_{D_s^{*-}} &= 2.112 \text{ GeV}. \end{aligned} \quad (19)$$

We use $C_D = 0.5 \pm 0.1$, $\omega = 0.1$ GeV for D/\bar{D} meson and $C_D = 0.4 \pm 0.1$, $\omega = 0.2$ GeV for D_s/\bar{D}_s meson, which are determined in Ref. [13] by fitting. In the wave function of $D_{(s)}^{(*)}$ mesons, the $\phi_{D^*}^L$ and $\phi_{D^*}^T$ can not be related by the equation of motion. We simply follow the authors in Ref. [17] and adopt the same model as that of D meson for them

$$\phi_{D^*}^L(x, b) = \phi_{D^*}^T(x, b) = \frac{1}{2\sqrt{2N_c}} f_{D^*} 6x(1-x)[1 + C_{D^*}(1-2x)] \exp\left[\frac{-(\omega^*)^2 b^2}{2}\right]. \quad (20)$$

The mass difference of $D_{(s)}$ and $D_{(s)}^*$ is very small. In a heavy quark limit, the light meson in $D_{(s)}^{(*)}$ mesons is not sensitive to the spin and color of the heavy c or \bar{c} quark. Thus the light-cone distribution amplitudes of $D_{(s)}$ and

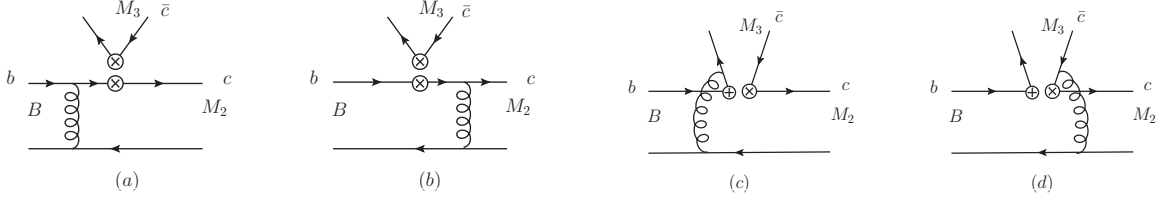


FIG. 1: Emission diagrams.

$D_{(s)}^*$ should be very similar. In our calculation, we simply take $C_{D^*} = C_D$ and $\omega^* = \omega$. $f_D = (207 \pm 4)$ MeV [21] and $f_{D_s} = (241 \pm 3)$ MeV [21] are adopted and the following relations derived from HQET [22] are used to determine $f_{D_{(s)}^*}$:

$$f_{D^*} = \sqrt{\frac{m_D}{m_{D^*}}} f_D, \quad f_{D_s^{*-}} = \sqrt{\frac{m_{D_s^-}}{m_{D_s^{*-}}}} f_{D_s^-}. \quad (21)$$

The value of f_{D_s} above is smaller than the recent experimental data $f_{D_s} = (273 \pm 10)$ MeV [18]. Because the amplitude in the PQCD approach is factorized as the convolution of the wave functions, Sudakov factors and the hard part, the branching ratio is proportional to the $f_{M_{2/3}}^2$. Thus if the experimental data is adopted, our results for the branching ratios will increase by $F = (\frac{273 \pm 10}{241 \pm 3})^2$ for single D_s meson in the final state and F^2 for double D_s meson final state.

D. Factorization Formulae for $B \rightarrow PP$ mode

In this subsection, we list all the amplitudes from the Feynman diagrams for $\langle M_2 M_3 | C_i(\mu) O_i(\mu) | B_{(s)} \rangle$ up to the leading order, with M_2 and M_3 as two charmed mesons. According to their topological structures, the diagrams that contribute to the decays of $B_{(s)}$ to two charmed mesons can be divided into two types, the emission diagrams (see Fig. 1) with the light antiquark in $B_{(s)}$ meson entering one of the charmed mesons as a spectator and the annihilation diagrams (see Figs. 2 and 3) without any spectator quark. The first two diagrams in Fig. 1 are factorizable diagrams, whose amplitude can be naively factorized as a decay constant of a charmed meson and a form factor like structure. The amplitudes arise from all the possible Lorentz structure of the operators for factorizable emission diagrams are given as following, where a_i denotes the Wilson coefficients and t is the scale.

- Factorizable emission diagrams for (V-A)(V-A) operator

$$F_e^{LL}(a_i(t)) = 8\pi C_F f_{M_3} m_B^4 \int_0^1 dx_1 dx_2 \int_0^{1/\Lambda} b_1 db_1 b_2 db_2 \phi_B(x_1, b_1) \phi_{M_2}(x_2) \\ \times \left[E_e(t_e^{(1)}) a_i(t_e^{(1)}) h_e(x_1, x_2(1 - r_3^2), b_1, b_2) S_t(x_2)(1 + x_2 + r_2(1 - 2x_2)) \right. \\ \left. + r_2(1 + r_2) E_e(t_e^{(2)}) a_i(t_e^{(2)}) h_e(x_2, x_1(1 - r_3^2), b_2, b_1) S_t(x_1) \right]. \quad (22)$$

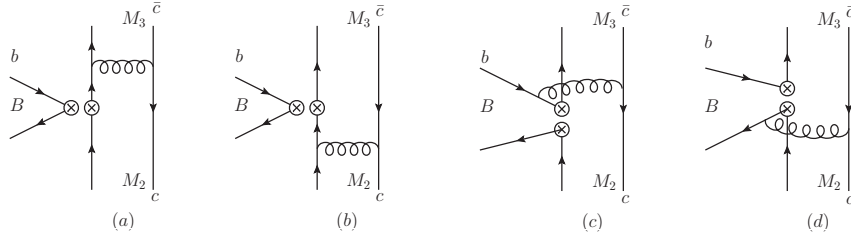


FIG. 2: Annihilation diagrams without charm quark in the four-quark operator.

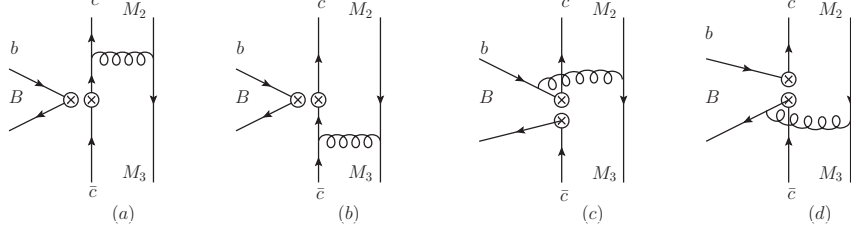


FIG. 3: Annihilation diagrams with charm quark in the four-quark operator.

- Factorizable emission diagrams for (S-P)(S+P) operator

$$\begin{aligned}
 F_e^{SP}(a_i(t)) &= 16\pi C_F f_{M_3} m_B^4 \int_0^1 dx_1 dx_2 \int_0^{1/\Lambda} b_1 db_1 b_2 db_2 \phi_B(x_1, b_1) \phi_{M_2}(x_2) \\
 &\quad \times r_3 \left[E_e(t_e^{(1)}) a_i(t_e^{(1)}) h_e(x_1, x_2(1-r_3^2), b_1, b_2) S_t(x_2) (1+2r_2+r_2x_2) \right. \\
 &\quad \left. + r_2 E_e(t_e^{(2)}) a_i(t_e^{(2)}) h_e(x_2, x_1(1-r_3^2), b_2, b_1) S_t(x_1) \right]. \quad (23)
 \end{aligned}$$

The amplitudes for the nonfactorizable emission diagrams in Fig.1(c) and (d) are given as:

- Nonfactorizable emission diagrams for (V-A)(V-A) operator are

$$\begin{aligned}
 F_{en}^{LL}(a_i(t)) &= 16\pi \sqrt{\frac{2}{3}} C_F m_B^4 \int_0^1 [dx] \int_0^{1/\Lambda} b_1 db_1 b_3 db_3 \phi_B(x_1, b_1) \phi_{M_2}(x_2) \phi_{M_3}(x_3) \\
 &\quad \times \left[(x_3 - r_2 x_2) E_b(t_{en}^{(1)}) a_i(t_{en}^{(1)}) h_{en}^{(1)}(x_i, b_i) \right. \\
 &\quad \left. + (x_2 r_2 - x_2 + x_3 - 1) E_{en}(t_{en}^{(2)}) a_i(t_{en}^{(2)}) h_{en}^{(2)}(x_i, b_i) \right]. \quad (24)
 \end{aligned}$$

- Nonfactorizable emission diagrams for (V-A)(V+A) operator are

$$\begin{aligned}
 F_{en}^{LR}(a_i(t)) &= 16\pi \sqrt{\frac{2}{3}} C_F m_B^4 \int_0^1 [dx] \int_0^{1/\Lambda} b_1 db_1 b_3 db_3 \phi_B(x_1, b_1) \phi_{M_2}(x_2) \phi_{M_3}(x_3) \\
 &\quad \times r_3 \left[(x_3 + r_2(x_2 + x_3)) E_{en}(t_{en}^{(1)}) a_i(t_{en}^{(1)}) h_{en}^{(1)}(x_i, b_i) \right. \\
 &\quad \left. - (r_2(x_2 - x_3 + 2) - x_3 + 2) E_{en}(t_{en}^{(2)}) a_i(t_{en}^{(2)}) h_{en}^{(2)}(x_i, b_i) \right]. \quad (25)
 \end{aligned}$$

The first two diagrams in Figs. 2 and 3 are the factorizable diagrams for annihilation diagrams, whose amplitudes can be factorized as a $B_{(s)}$ meson decay constant and a form factor like structure between two charmed mesons. It

should be reminded that, in the decays we considered, the factorizable annihilation diagrams can be divided into two types, depending on whether the quark propagator is a light quark propagator (see the first two diagrams in Fig. 2) or a c -quark propagator (see the first diagrams in Fig. 3). In calculation we keep the mass of the c -quark while the mass of the light quark is neglected and thus these two types of diagrams have different expressions. The amplitudes for the factorizable annihilation diagrams with a light quark propagator (the first two diagrams in Fig. 2) are given as follows:

- Factorizable annihilation diagrams for (V-A)(V-A) operator

$$\begin{aligned}
F_a^{LL}(a_i(t)) &= 8\pi C_F f_B m_B^4 \int_0^1 dx_2 dx_3 \int_0^{1/\Lambda} b_2 db_2 b_3 db_3 \phi_{M_2}(x_2) \phi_{M_3}(x_3) \\
&\times [(2r_2 r_3 (x_2 - 2) + x_2 - 1) \\
&\times E_a(t_a^{(1)}) a_i(t_a^{(1)}) h_a(1 - (1 - r_2^2)x_3, 1 - (1 - r_3^2)x_2, b_3, b_2) S_t(x_2) \\
&+ (-2r_2 r_3 (x_3 - 2) - (x_3 - 1)) \\
&\times E_a(t_a^{(2)}) a_i(t_a^{(2)}) h_a(1 - (1 - r_3^2)x_2, 1 - (1 - r_2^2)x_3, b_2, b_3) S_t(x_3)] . \quad (26)
\end{aligned}$$

The two terms of $F_a^{LL}(a_i(t))$ give destructive contributions. Very little contribution appears when ϕ_{M_2} and ϕ_{M_3} are different from each other. Otherwise, $F_a^{LL}(a_i(t)) = 0$.

- Factorizable annihilation diagrams for (V-A)(V+A) operator

$$F_a^{LR}(a_i(t)) = F_a^{LL}(a_i(t)). \quad (27)$$

- Factorizable annihilation diagrams for (S-P)(S+P) operator

$$\begin{aligned}
F_a^{SP}(a_i(t)) &= 16\pi C_F f_B m_B^4 \int_0^1 dx_2 dx_3 \int_0^{1/\Lambda} b_2 db_2 b_3 db_3 \phi_{M_2}(x_2) \phi_{M_3}(x_3) \\
&\times [(2r_3 + r_2(1 - x_2)) E_a(t_a^{(1)}) a_i(t_a^{(1)}) h_a(1 - (1 - r_2^2)x_3, 1 - (1 - r_3^2)x_2, b_3, b_2) S_t(x_2) \\
&+ (2r_2 + r_3(1 - x_3)) E_a(t_a^{(2)}) a_i(t_a^{(2)}) h_a(1 - (1 - r_3^2)x_2, 1 - (1 - r_2^2)x_3, b_2, b_3) S_t(x_3)] . \quad (28)
\end{aligned}$$

For the amplitudes of the factorizable diagrams with a c -quark propagator (the first two diagrams in Fig. 3), we add the character ‘‘c’’ in the subscript to distinguish them from those with a light quark propagator. Because of current conservation, the factorizable annihilation diagrams of $B \rightarrow PP$ decay mode for (V-A)(V-A) and (V-A)(V+A) operators cancel each other. Amplitudes for these diagrams are given as follows:

- Factorizable annihilation diagrams for (V-A)(V-A) operator

$$F_{ac}^{LL}(a_i(t)) = 0 . \quad (29)$$

- Factorizable annihilation diagrams for (V-A)(V+A) operator

$$F_{ac}^{LR}(a_i(t)) = F_{ac}^{LL}(a_i(t)) = 0. \quad (30)$$

Similar to the factorizable annihilation diagrams, the nonfactorizable annihilation diagrams are also divided into two types (see the last two diagrams of Figs. 2 and 3), depending on whether the $c\bar{c}$ are generated from the effective weak vertex. Because the c quark in the charmed meson carries most of the energy, these two types of nonfactorizable diagrams are expected to have different scales. Additionally, because the momentum fraction $x_i (i = 2, 3)$ is defined on the light quark in the charmed mesons, these two types of nonfactorizable annihilation diagrams also have different expressions. The amplitudes of the diagrams with $c\bar{c}$ pair generated from a hard gluon (the last two diagrams in Fig. 2) are given as

- Nonfactorizable annihilation diagrams for (V-A)(V-A) operator

$$\begin{aligned}
F_{an}^{LL}(a_i(t)) &= 16\pi\sqrt{\frac{2}{3}}C_F m_B^4 \int_0^1 [dx] \int_0^{1/\Lambda} b_1 db_1 b_2 db_2 \phi_B(x_1, b_1) \phi_{M_2}(x_2) \phi_{M_3}(x_3) \\
&\quad \times \left[(r_2 r_3 (x_2 + x_3 - 4) + x_3 - 1) E_{an}(t_{an}^{(1)}) a_i(t_{an}^{(1)}) h_{an}^{(1)}(x_i, b_i) \right. \\
&\quad \left. - (r_2 r_3 (x_2 + x_3 - 2) + x_2 - 1) E_{an}(t_{an}^{(2)}) a_i(t_{an}^{(2)}) h_{an}^{(2)}(x_i, b_i) \right]. \tag{31}
\end{aligned}$$

- Nonfactorizable annihilation diagrams for (V-A)(V+A) operator

$$\begin{aligned}
F_{an}^{LR}(a_i(t)) &= 16\pi\sqrt{\frac{2}{3}}C_F m_B^4 \int_0^1 [dx] \int_0^{1/\Lambda} b_1 db_1 b_2 db_2 \phi_B(x_1, b_1) \phi_{M_2}(x_2) \phi_{M_3}(x_3) \\
&\quad \times \left[-(r_2(x_2 + 1) - r_3(x_3 + 1)) E_{an}(t_{an}^{(1)}) a_i(t_{an}^{(1)}) h_{an}^{(1)}(x_i, b_i) \right. \\
&\quad \left. + (r_2(x_2 - 1) - r_3(x_3 - 1)) E_{an}(t_{an}^{(2)}) a_i(t_{an}^{(2)}) h_{an}^{(2)}(x_i, b_i) \right]. \tag{32}
\end{aligned}$$

- Nonfactorizable annihilation diagrams for (S-P)(S+P) operator

$$\begin{aligned}
F_{an}^{SP}(a_i(t)) &= 16\pi\sqrt{\frac{2}{3}}C_F m_B^4 \int_0^1 [dx] \int_0^{1/\Lambda} b_1 db_1 b_2 db_2 \phi_B(x_1, b_1) \phi_{M_2}(x_2) \phi_{M_3}(x_3) \\
&\quad \times \left[(r_2 r_3 (x_2 + x_3 - 4) + x_2 - 1) E_{an}(t_{an}^{(1)}) a_i(t_{an}^{(1)}) h_{an}^{(1)}(x_i, b_i) \right. \\
&\quad \left. - (r_2 r_3 (x_2 + x_3 - 2) + x_3 - 1) E_{an}(t_{an}^{(2)}) a_i(t_{an}^{(2)}) h_{an}^{(2)}(x_i, b_i) \right]. \tag{33}
\end{aligned}$$

Similar to what we do with the factorizable annihilation diagrams, the amplitudes with $c\bar{c}$ pair from the effective weak vertex are also distinguished by adding the character “c” in the subscripts. Amplitudes for these diagrams (the last two diagrams in Fig. 3) are given by

- Nonfactorizable annihilation diagrams for (V-A)(V-A) operator

$$\begin{aligned}
F_{anc}^{LL}(a_i(t)) &= 16\pi\sqrt{\frac{2}{3}}C_F m_B^4 \int_0^1 [dx] \int_0^{1/\Lambda} b_1 db_1 b_2 db_2 \phi_B(x_1, b_1) \phi_{M_2}(x_2) \phi_{M_3}(x_3) \\
&\quad \times \left[(-r_2 r_3 (x_2 + x_3 + 2) - x_2) E_{an}(t_{an}^{(1c)}) a_i(t_{an}^{(1c)}) h_{an}^{(1c)}(x_i, b_i) \right. \\
&\quad \left. + (r_2 r_3 (x_2 + x_3) + x_3) E_{an}(t_{an}^{(2c)}) a_i(t_{an}^{(2c)}) h_{an}^{(2c)}(x_i, b_i) \right]. \tag{34}
\end{aligned}$$

- Nonfactorizable annihilation diagrams for (S-P)(S+P) operator

$$\begin{aligned}
F_{anc}^{SP}(a_i(t)) &= 16\pi\sqrt{\frac{2}{3}}C_F m_B^4 \int_0^1 [dx] \int_0^{1/\Lambda} b_1 db_1 b_2 db_2 \phi_B(x_1, b_1) \phi_{M_2}(x_2) \phi_{M_3}(x_3) \\
&\quad \times \left[-(r_2 r_3 (x_2 + x_3 + 2) + x_3) E_{an}(t_{an}^{(1c)}) a_i(t_{an}^{(1c)}) h_{an}^{(1c)}(x_i, b_i) \right. \\
&\quad \left. + ((r_2 r_3 + 1)x_2 + r_3 x_3 (r_2 + r_3)) E_{an}(t_{an}^{(2c)}) a_i(t_{an}^{(2c)}) h_{an}^{(2c)}(x_i, b_i) \right]. \tag{35}
\end{aligned}$$

E. Analytic expressions for the decay amplitudes

There are 10 decay channels for the $B \rightarrow PP$ decay mode, which can be divided into two groups: decays with both emission and annihilation contributions and pure annihilation type decays.

- Channels with both emission and annihilation contributions.

$$\begin{aligned} \mathcal{A}(B^- \rightarrow D^0 D_{(s)}^-) &= \frac{G_F}{\sqrt{2}} \left\{ V_{cb} V_{cd(s)}^* [F_e^{LL}(a_1) + F_{en}^{LL}(C_1)] + V_{ub} V_{ud(s)}^* [F_a^{LL}(a_1) + F_{an}^{LL}(C_1)] \right. \\ &\quad - V_{tb} V_{td(s)}^* [F_e^{LL}(a_4 + a_{10}) + F_{en}^{LL}(C_3 + C_9) + F_e^{SP}(a_6 + a_8) + F_{en}^{LR}(C_5 + C_7) \\ &\quad \left. + F_a^{LL}(a_4 + a_{10}) + F_{an}^{LL}(C_3 + C_9) + F_a^{SP}(a_6 + a_8) + F_{an}^{LR}(C_5 + C_7)] \right\}, \quad (36) \end{aligned}$$

$$\begin{aligned} \mathcal{A}(\bar{B}^0 \rightarrow D^+ D^-) &= \frac{G_F}{\sqrt{2}} \left\{ V_{cb} V_{cd}^* [F_e^{LL}(a_1) + F_{en}^{LL}(C_1) + F_{ac}^{LL}(a_2) + F_{anc}^{LL}(C_2)] \right. \\ &\quad - V_{tb} V_{td}^* [F_e^{LL}(a_4 + a_{10}) + F_{en}^{LL}(C_3 + C_9) + F_e^{SP}(a_6 + a_8) + F_{en}^{LR}(C_5 + C_7) \\ &\quad + F_{ac}^{LL}(a_3 + a_9) + F_{anc}^{LL}(C_4 + C_{10}) + F_{ac}^{LR}(a_5 + a_7) + F_{anc}^{SP}(C_6 + C_8) \\ &\quad + F_a^{LL}(a_3 + a_4 - \frac{1}{2}a_9 - \frac{1}{2}a_{10}) + F_{an}^{LL}(C_3 + C_4 - \frac{1}{2}C_9 - \frac{1}{2}C_{10}) \\ &\quad \left. + F_a^{LR}(a_5 - \frac{1}{2}a_7) + F_{an}^{SP}(C_6 - \frac{1}{2}C_8) + F_a^{SP}(a_6 - \frac{1}{2}a_8) + F_{an}^{LR}(C_5 - \frac{1}{2}C_7)] \right\}, \quad (37) \end{aligned}$$

$$\begin{aligned} \mathcal{A}(\bar{B}^0 \rightarrow D^+ D_s^-) &= \frac{G_F}{\sqrt{2}} \left\{ V_{cb} V_{cs}^* [F_e^{LL}(a_1) + F_{en}^{LL}(C_1)] - V_{tb} V_{ts}^* [F_e^{LL}(a_4 + a_{10}) + F_{en}^{LL}(C_3 + C_9) \right. \\ &\quad + F_e^{SP}(a_6 + a_8) + F_{en}^{LR}(C_5 + C_7) + F_a^{LL}(a_4 - \frac{1}{2}a_{10}) + F_{an}^{LL}(C_3 - \frac{1}{2}C_9) \\ &\quad \left. + F_a^{SP}(a_6 - \frac{1}{2}a_8) + F_{an}^{LR}(C_5 - \frac{1}{2}C_7)] \right\}, \quad (38) \end{aligned}$$

$$\begin{aligned} \mathcal{A}(\bar{B}_s^0 \rightarrow D_s^+ D^-) &= \frac{G_F}{\sqrt{2}} \left\{ V_{cb} V_{cd}^* [F_e^{LL}(a_1) + F_{en}^{LL}(C_1)] - V_{tb} V_{td}^* [F_e^{LL}(a_4 + a_{10}) + F_{en}^{LL}(C_3 + C_9) \right. \\ &\quad + F_e^{SP}(a_6 + a_8) + F_{en}^{LR}(C_5 + C_7) + F_a^{LL}(a_4 - \frac{1}{2}a_{10}) + F_{an}^{LL}(C_3 - \frac{1}{2}C_9) \\ &\quad \left. + F_a^{SP}(a_6 - \frac{1}{2}a_8) + F_{an}^{LR}(C_5 - \frac{1}{2}C_7)] \right\}, \quad (39) \end{aligned}$$

$$\begin{aligned} \mathcal{A}(\bar{B}_s^0 \rightarrow D_s^+ D_s^-) &= \frac{G_F}{\sqrt{2}} \left\{ V_{cb} V_{cs}^* [F_e^{LL}(a_1) + F_{en}^{LL}(C_1) + F_{ac}^{LL}(a_2) + F_{anc}^{LL}(C_2)] \right. \\ &\quad - V_{tb} V_{ts}^* [F_e^{LL}(a_4 + a_{10}) + F_{en}^{LL}(C_3 + C_9) + F_e^{SP}(a_6 + a_8) + F_{en}^{LR}(C_5 + C_7) \\ &\quad + F_{ac}^{LL}(a_3 + a_9) + F_{anc}^{LL}(C_4 + C_{10}) + F_{ac}^{LR}(a_5 + a_7) + F_{anc}^{SP}(C_6 + C_8) \\ &\quad + F_a^{LL}(a_3 + a_4 - \frac{1}{2}a_9 - \frac{1}{2}a_{10}) + F_{an}^{LL}(C_3 + C_4 - \frac{1}{2}C_9 - \frac{1}{2}C_{10}) \\ &\quad \left. + F_a^{LR}(a_5 - \frac{1}{2}a_7) + F_{an}^{SP}(C_6 - \frac{1}{2}C_8) + F_a^{SP}(a_6 - \frac{1}{2}a_8) + F_{an}^{LR}(C_5 - \frac{1}{2}C_7)] \right\}, \quad (40) \end{aligned}$$

- Pure annihilation decays.

$$\begin{aligned} \mathcal{A}(\bar{B}^0 \rightarrow D^0 \bar{D}^0) &= \frac{G_F}{\sqrt{2}} \left\{ V_{cb} V_{cd}^* [F_{ac}^{LL}(a_2) + F_{anc}^{LL}(C_2)] + V_{ub} V_{ud}^* [F_a^{LL}(a_2) + F_{an}^{LL}(C_2)] \right. \\ &\quad - V_{tb} V_{td}^* [F_a^{LL}(a_3 + a_9) + F_{an}^{LL}(C_4 + C_{10}) + F_a^{LR}(a_5 + a_7) + F_{an}^{SP}(C_6 + C_8) \\ &\quad \left. + F_{ac}^{LL}(a_3 + a_9) + F_{anc}^{LL}(C_4 + C_{10}) + F_{ac}^{LR}(a_5 + a_7) + F_{anc}^{SP}(C_6 + C_8)] \right\}, \quad (41) \end{aligned}$$

$$\begin{aligned}
\mathcal{A}(\bar{B}^0 \rightarrow D_s^+ D_s^-) &= \frac{G_F}{\sqrt{2}} \left\{ V_{cb} V_{cd}^* [F_{ac}^{LL}(a_2) + F_{anc}^{LL}(C_2)] - V_{tb} V_{td}^* [F_{ac}^{LL}(a_3 + a_9) + F_{anc}^{LL}(C_4 + C_{10})] \right. \\
&\quad + F_{ac}^{LR}(a_5 + a_7) + F_{anc}^{SP}(C_6 + C_8) + F_a^{LL}(a_3 - \frac{1}{2}a_9) + F_{an}^{LL}(C_4 - \frac{1}{2}C_{10}) \\
&\quad \left. + F_a^{LR}(a_5 - \frac{1}{2}a_7) + F_{an}^{SP}(C_6 - \frac{1}{2}C_8) \right\}, \tag{42}
\end{aligned}$$

$$\begin{aligned}
\mathcal{A}(\bar{B}_s^0 \rightarrow D^0 \bar{D}^0) &= \frac{G_F}{\sqrt{2}} \left\{ V_{cb} V_{cs}^* [F_{ac}^{LL}(a_2) + F_{anc}^{LL}(C_2)] + V_{ub} V_{us}^* [F_a^{LL}(a_2) + F_{an}^{LL}(C_2)] \right. \\
&\quad - V_{tb} V_{ts}^* [F_a^{LL}(a_3 + a_9) + F_{an}^{LL}(C_4 + C_{10}) + F_a^{LR}(a_5 + a_7) + F_{an}^{SP}(C_6 + C_8)] \\
&\quad \left. + F_{ac}^{LL}(a_3 + a_9) + F_{anc}^{LL}(C_4 + C_{10}) + F_{ac}^{LR}(a_5 + a_7) + F_{anc}^{SP}(C_6 + C_8) \right\}, \tag{43}
\end{aligned}$$

$$\begin{aligned}
\mathcal{A}(\bar{B}_s^0 \rightarrow D^+ D^-) &= \frac{G_F}{\sqrt{2}} \left\{ V_{cb} V_{cs}^* [F_{ac}^{LL}(a_2) + F_{anc}^{LL}(C_2)] - V_{tb} V_{ts}^* [F_{ac}^{LL}(a_3 + a_9) + F_{anc}^{LL}(C_4 + C_{10})] \right. \\
&\quad + F_{ac}^{LR}(a_5 + a_7) + F_{anc}^{SP}(C_6 + C_8) + F_a^{LL}(a_3 - \frac{1}{2}a_9) + F_{an}^{LL}(C_4 - \frac{1}{2}C_{10}) \\
&\quad \left. + F_a^{LR}(a_5 - \frac{1}{2}a_7) + F_{an}^{SP}(C_6 - \frac{1}{2}C_8) \right\}. \tag{44}
\end{aligned}$$

There are also 10 decay channels for each category of $B \rightarrow PV$, $B \rightarrow VP$, and $B \rightarrow VV$ decays. The decay amplitudes of the $B \rightarrow PV$ and $B \rightarrow VP$ modes can be obtained from the $B \rightarrow PP$ decays just by substituting the $D_{(s)}/\bar{D}_{(s)}$ meson for the corresponding $D_{(s)}^*/\bar{D}_{(s)}^*$ meson. The factorization formulae for these two decay modes are listed in Appendix B and C, respectively.

The amplitude of $B \rightarrow VV$ decay can be decomposed as

$$\mathcal{A}(\epsilon_2, \epsilon_3) = i\mathcal{A}^N + i(\epsilon_{2T}^* \cdot \epsilon_{3T}^*)\mathcal{A}^s + (\epsilon_{\mu\nu\alpha\beta} n^\mu \bar{n}^\nu \epsilon_{2T}^{*\alpha} \epsilon_{3T}^{*\beta})\mathcal{A}^p, \tag{45}$$

where \mathcal{A}^N , including the D wave and part of the S wave component, contains the contribution from the longitudinal polarizations \mathcal{A}^s and \mathcal{A}^p , corresponding to part of the S wave component and all the P wave component, respectively, which represent the transversely polarized contributions, and they have the following relationships with the helicity amplitudes (an i in the amplitude is dropped):

$$A_0 = \mathcal{A}^N, \quad A_\pm = \mathcal{A}^s \pm \mathcal{A}^p. \tag{46}$$

For each decay process of $B \rightarrow VV$, the amplitudes \mathcal{A}^N , \mathcal{A}^s , and \mathcal{A}^p have the same structures as Eq.(36)-(44), respectively. The factorization formulae for the longitudinal and transverse polarization for the $B \rightarrow VV$ decays are all listed in Appendix D.

III. NUMERICAL ANALYSIS

The decay widths of B to two charmed mesons decays can be directly derived from the formulas of two-body decays in Ref. [18]. With the amplitude obtained in Sec. II, the decay widths for the $B \rightarrow PP$, $B \rightarrow PV$, and $B \rightarrow VP$ decays are given by

$$\Gamma = \frac{[(1 - (r_2 + r_3)^2)(1 - (r_2 - r_3)^2)]^{1/2}}{16\pi m_B} |\mathcal{A}|^2. \tag{47}$$

For the $B \rightarrow VV$ decays, the decay width is given by

$$\Gamma = \frac{[(1 - (r_2 + r_3)^2)(1 - (r_2 - r_3)^2)]^{1/2}}{16\pi m_B} \sum_{i=0,+,-} |A_i|^2. \quad (48)$$

The branching ratio is given by $\mathcal{BR} = \Gamma\tau_B$.

The key observables of the decays related in this paper are the CP averaged branching ratios as well as direct CP asymmetries($A_{\text{CP}}^{\text{dir}}$) and mixing induced CP asymmetries($A_{\text{CP}}^{\text{mix}}$). Readers are referred to Ref. [19] for some reviews on CP violation. First, we define four amplitudes as follows:

$$\begin{aligned} A_f &= \langle f | \mathcal{H} | B \rangle, & \bar{A}_f &= \langle f | \mathcal{H} | \bar{B} \rangle, \\ A_{\bar{f}} &= \langle \bar{f} | \mathcal{H} | B \rangle, & \bar{A}_{\bar{f}} &= \langle \bar{f} | \mathcal{H} | \bar{B} \rangle, \end{aligned} \quad (49)$$

where \bar{B} meson has a b quark in it and \bar{f} is the CP conjugate state of f . The direct CP asymmetry $A_{\text{CP}}^{\text{dir}}$ is defined by

$$A_{\text{CP}}^{\text{dir}} = \frac{|\bar{A}_{\bar{f}}|^2 - |A_f|^2}{|\bar{A}_{\bar{f}}|^2 + |A_f|^2}. \quad (50)$$

In neutral B meson decays, if the final states are CP eigen states $f = \bar{f}$, the time-dependent CP asymmetry with mixing effects present, is defined by

$$\begin{aligned} A_{\text{CP}}(B(t) \rightarrow f) &\equiv \frac{\Gamma(B(t) \rightarrow f) - \Gamma(\bar{B}(t) \rightarrow f)}{\Gamma(B(t) \rightarrow f) + \Gamma(\bar{B}(t) \rightarrow f)} \\ &= -C_f \cos(\Delta Mt) + A_{\text{CP}}^{\text{mix}}(B \rightarrow f) \sin(\Delta Mt), \end{aligned} \quad (51)$$

where ΔM is the mass difference of B meson mass eigenstates. After some calculation, we can get the explicit expressions

$$\begin{aligned} C_f &= \frac{|A_f|^2 - |\bar{A}_f|^2}{|A_f|^2 + |\bar{A}_f|^2}, \\ A_{\text{CP}}^{\text{mix}} &= \frac{2\text{Im}[\frac{q}{p}\bar{A}_f A_f^*]}{|A_f|^2 + |\bar{A}_f|^2}. \end{aligned} \quad (52)$$

Since the mixing CP violation in neutral B meson system is negligible in a good approximation, we have

$$\frac{q}{p} = e^{-i\phi_{M(B)}} = \frac{V_{tb}^* V_{t(d/s)}}{V_{tb} V_{t(d/s)}^*}. \quad (53)$$

Our results for CP averaged branching ratios and CP asymmetries are listed in Tables I, II, III, IV, and V. All the experimental data are from the Particle Data Group[18] except the ones marked with ‘‘BaBar’’ and ‘‘Belle’’. In Table IV, we also list the ratios of the transverse polarizations \mathcal{R}_T in the branching ratios for $B \rightarrow VV$ decays, which is defined by

$$\mathcal{R}_T = \frac{|A_+|^2 + |A_-|^2}{|A_0|^2 + |A_+|^2 + |A_-|^2}. \quad (54)$$

The first errors in our results are estimated from the hadronic parameters: (1) The decay constants of $B_{(s)}$ mesons: $f_B = (0.19 \pm 0.025)\text{GeV}$ for B mesons and $f_{B_s} = (0.23 \pm 0.03)\text{GeV}$ for B_s meson; (2) The shape parameters in $B_{(s)}$ meson wave functions: $\omega_b = (0.40 \pm 0.05)\text{GeV}$ for B meson and $\omega_{b_s} = (0.50 \pm 0.05)\text{GeV}$ for B_s meson; (3)

The decay constants and the shape parameters in the wave functions of charmed mesons, which are given in the last paragraph in Sec. II C. The second errors are from the not known next-to-leading order QCD corrections with respect to α_s and nonperturbative power corrections with respect to scales in Eq.(7), characterized by the choice of the $\Lambda_{\text{QCD}} = (0.25 \pm 0.05)\text{GeV}$ and the variations of the factorization scales shown in Appendix A. The third errors are brought in by the CKM matrix elements, which are given as[20]

$$\begin{aligned}
|V_{cb}| &= 0.041\ 17_{-0.001\ 15}^{+0.000\ 38}, & |V_{cd}| &= 0.225\ 08_{-0.000\ 82}^{+0.000\ 82}, & |V_{cs}| &= 0.973\ 47_{-0.000\ 19}^{+0.000\ 19}, \\
|V_{ub}| &= 0.003\ 5_{-0.000\ 14}^{+0.000\ 15}, & |V_{ud}| &= 0.974\ 44_{-0.000\ 28}^{+0.000\ 28}, & |V_{us}| &= 0.225\ 7_{-0.001\ 1}^{+0.001\ 1}, \\
|V_{tb}| &= 0.999\ 146_{-0.000\ 016}^{+0.000\ 047}, & |V_{td}| &= 0.008\ 59_{-0.000\ 29}^{+0.000\ 27}, & |V_{ts}| &= 0.040\ 41_{-0.001\ 15}^{+0.000\ 38}, \\
\gamma &= (67.8_{-3.9}^{+4.2})^\circ, & \beta &= (21.58_{-0.81}^{+0.91})^\circ.
\end{aligned} \tag{55}$$

The other input parameters are [18]

$$\begin{aligned}
G_F &= 1.16639 \times 10^{-5} \text{GeV}^{-2}, \\
\tau_{B^-} &= 1.639 \times 10^{-12} \text{s}/\hbar, \quad \tau_{B^0} = 1.530 \times 10^{-12} \text{s}/\hbar, \quad \tau_{B_s^0} = 1.478 \times 10^{-12} \text{s}/\hbar, \\
m_B &= 5.28 \text{GeV}, \quad m_{B_s} = 5.366 \text{GeV}, \quad m_D = 1.87 \text{GeV}, \quad m_{D_s} = 1.97 \text{GeV}, \\
m_{D^*} &= 2.01 \text{GeV}, \quad m_{D_s^*} = 2.11 \text{GeV}, \quad \hbar = 6.582119 \times 10^{-25} \text{GeV s}.
\end{aligned} \tag{56}$$

Because in the direct CP asymmetries the errors arising from the CKM elements are very small, we neglect them. In the $B \rightarrow VV$ decays, the ratios of the transverse polarizations' contributions (\mathcal{R}_T) are not very sensitive to the parameters listed above. The next-to-leading order corrections on r occur at the $r^2 = 0.13$ order and thus the errors from the higher orders of r are very small except for \mathcal{R}_T . This is confirmed at the numerical calculations. Therefore we only keep these errors in \mathcal{R}_T and neglect them in other physical quantities. We will talk about the errors of these ratios later.

The first 6 channels in each of Tables I, II, III, IV and V, receive contributions from both emission diagrams and annihilation diagrams; while the last 4 channels in each table are pure annihilation processes. In order to make our discussions easier, we give a number to each channel in the beginning of each line in the tables.

Compared with the tree operators, the penguin operators give very small contributions because of the severe suppression of the Wilson coefficients. By calculating the ratio of the branching fraction with only penguin contributions and that with all contributions in the same channel, we estimate how much the penguin operators contribute. Our results show that the penguin operators contribute 0.1% – 0.2% in those channels with a W emission contribution, and contribute 0.3% – 0.7% in those pure annihilation processes. Thus it is enough to pay our attention only to the tree operators in the following for the investigation of the branching ratios. Different from the counting rules of the PQCD calculation of B to two light mesons decays, the nonfactorizable emission diagrams may give large contributions because the asymmetry of the two quarks in charmed mesons can not make the two diagrams nearly cancel each other. However, from Eq.(36)-Eq.(44), one can find that the contributions of the nonfactorizable emission diagrams are suppressed by the small Wilson coefficient C_1 . Since the charm quark is heavier than the u, d, s quark, the gluons in Fig. 3 are softer than those in Fig. 2. This indicates that the diagrams in Fig. 3 will give larger contributions than

TABLE I: CP averaging branching ratios (unit: 10^{-4}) and the CP asymmetries for $B \rightarrow PP$ decays.

Channels	\mathcal{BR}		$A_{CP}^{\text{dir}}(\%)$		A_{CP}^{mix}	
	Exp.	This work	Exp.	This work	Exp.	This work
1 $B^- \rightarrow D^0 D^-$	4.2 ± 0.6	$3.9_{-1.9-1.1-0.2}^{+2.9+0.7+0.1}$	$-13 \pm 14 \pm 2$	$0.6_{-0.0-0.1}^{+0.4+0.4}$...	
2 $B^- \rightarrow D^0 D_s^-$	103 ± 17	$95_{-46-26-6}^{+69+18+2}$	$\sim -10^{-3}$...	
3 $\bar{B}^0 \rightarrow D^+ D^-$	2.11 ± 0.31	$3.7_{-1.8-0.9-0.2}^{+2.9+0.4+0.1}$	$11 \pm 22 \pm 7[\text{Babar}]$ $-91 \pm 23 \pm 6[\text{Belle}]$	$0.5_{-0.2-0.4}^{+0.1+0.5}$	-0.81 ± 0.29	$-0.73_{-0.00-0.01-0.02}^{+0.00+0.01+0.02}$
4 $\bar{B}^0 \rightarrow D^+ D_s^-$	74 ± 7	$89_{-43-25-5}^{+68+18+2}$	
5 $\bar{B}_s^0 \rightarrow D_s^+ D^-$		$2.2_{-1.0-0.7-0.1}^{+1.4+0.7+0.1}$	$0.5_{-0.0-0.1}^{+0.1+0.2}$...	
6 $\bar{B}_s^0 \rightarrow D_s^+ D_s^-$	110 ± 40	$55_{-24-15-3}^{+36+12+1}$	
7 $\bar{B}^0 \rightarrow D^0 \bar{D}^0$	$< 0.6[\text{BaBar}]$	$0.28_{-0.11-0.08-0.02}^{+0.07+0.03+0.01}$	$-5.3_{-2.7-3.3-0.3}^{+0.2+0.0+0.2}$		$-0.74_{-0.01-0.01-0.02}^{+0.00+0.00+0.02}$	
8 $\bar{B}^0 \rightarrow D_s^+ D_s^-$	$< 0.36[\text{Belle}]$	$0.35_{-0.13-0.10-0.02}^{+0.12+0.07+0.01}$	$-2.3_{-0.4-0.4}^{+0.5+0.8}$		$-0.73_{-0.00-0.01-0.02}^{+0.00+0.00+0.02}$	
9 $\bar{B}_s^0 \rightarrow D^0 \bar{D}^0$		$5.0_{-1.5-1.2-0.3}^{+1.7+1.0+0.1}$	$0.2_{-0.0-0.0}^{+0.1+0.1}$		$\sim 10^{-3}$	
10 $\bar{B}_s^0 \rightarrow D^+ D^-$		$5.2_{-1.9-1.4-0.3}^{+1.5+0.7+0.1}$	

TABLE II: CP averaging branching ratios (unit: 10^{-4}) and the CP asymmetries for $B \rightarrow PV$ decays.

Channels	\mathcal{BR}		$A_{CP}^{\text{dir}}(\%)$	
	Exp.	This work	Exp.	This work
1 $B^- \rightarrow D^0 D^{*-}$	3.9 ± 0.5	$3.6_{-1.7-1.0-0.2}^{+2.6+0.7+0.1}$	$0.1_{-0.1-0.1}^{+0.4+0.1}$	
2 $B^- \rightarrow D^0 D_s^{*-}$	78 ± 16	$89_{-42-24-5}^{+64+20+2}$	$\sim -10^{-3}$	
3 $\bar{B}^0 \rightarrow D^+ D^{*-}$	6.1 ± 1.5	$3.2_{-1.5-0.8-0.2}^{+2.4+0.5+0.1}$	-6 ± 9	$\sim 10^{-2}$
4 $\bar{B}^0 \rightarrow D^+ D_s^{*-}$	76 ± 16	$83_{-39-23-5}^{+61+17+2}$...	
5 $\bar{B}_s^0 \rightarrow D_s^+ D^{*-}$		$2.1_{-0.9-0.7-0.1}^{+1.3+0.7+0.0}$	$0.1_{-0.1-0.0}^{+0.0+0.0}$	
6 $\bar{B}_s^0 \rightarrow D_s^+ D_s^{*-}$		$48_{-21-15-3}^{+31+15+1}$...	
7 $\bar{B}^0 \rightarrow D^0 \bar{D}^{*0}$	$< 2.9[\text{Babar}][25]$	$(4.6_{-1.7-1.4-0.2}^{+1.5+1.3+0.9}) \times 10^{-2}$	$-4.1_{-4.4-2.9}^{+1.3+0.0}$	
8 $\bar{B}^0 \rightarrow D_s^+ D_s^{*-}$	$< 1.3[\text{BaBar}][24]$	$(3.5_{-1.2-1.1-0.2}^{+1.4+1.8+0.1}) \times 10^{-2}$	$0.5_{-0.3-0.7}^{+0.1+1.7}$	
9 $\bar{B}_s^0 \rightarrow D^0 \bar{D}^{*0}$		$0.83_{-0.24-0.19-0.04}^{+0.41+0.32+0.01}$	$0.4_{-0.2-0.1}^{+0.1+0.1}$	
10 $\bar{B}_s^0 \rightarrow D^+ D^{*-}$		$0.74_{-0.29-0.23-0.04}^{+0.23+0.24+0.01}$...	

those in Fig. 2. It is confirmed by our numerical results. However, these contributions are still much smaller than those from the factorizable emission diagrams. Thus, the branching ratios of the first 6 channels in Tables I, II, III, and IV are dominated by the factorizable emission diagrams.

Because the factorizable emission diagrams are dominate, the amplitude of the first 6 channels in each table should be nearly proportional to the product of a decay constant and a $B \rightarrow D$ transition form factor. Based on this physical picture, we can have the following simple conclusions:

TABLE III: CP averaging branching ratios (unit: 10^{-4}) and the CP asymmetries for $B \rightarrow VP$ (characterized by $B \rightarrow V$ form factor) decays.

Channels	\mathcal{BR}		$A_{CP}^{\text{dir}}(\%)$	
	Exp.	This work	Exp.	This work
1 $B^- \rightarrow D^{*0} D^-$	$6.3 \pm 1.4 \pm 1.0$ [BaBar][25]	$4.8^{+3.4+1.1+0.1}_{-2.3-1.4-0.3}$	$-0.5^{+0.1+0.0}_{-0.2-0.3}$	
2 $B^- \rightarrow D^{*0} D_s^-$	84 ± 17	$119^{+94+27+2}_{-56-34-7}$	$\sim -10^{-3}$	
3 $\bar{B}^0 \rightarrow D^{*+} D^-$	8.8 ± 1.6	$4.6^{+3.5+0.9+0.1}_{-2.1-1.1-0.3}$	$-0.6^{+0.0+0.1}_{-0.1-0.2}$	
4 $\bar{B}^0 \rightarrow D^{*+} D_s^-$	83 ± 11	$112^{+86+26+2}_{-53-32-6}$...	
5 $\bar{B}_s^0 \rightarrow D_s^{*+} D^-$		$2.7^{+1.7+0.9+0.1}_{-1.1-0.9-0.1}$	$-0.4^{+0.0+0.1}_{-0.0-0.1}$	
6 $\bar{B}_s^0 \rightarrow D_s^{*+} D_s^-$		$70^{+44+19+1}_{-31-21-4}$...	
7 $\bar{B}^0 \rightarrow D^{*0} \bar{D}^0$		$0.21^{+0.06+0.03+0.00}_{-0.08-0.05-0.01}$	$-1.2^{+0.3+0.7+0.1}_{-1.2-1.4-0.1}$	
8 $\bar{B}^0 \rightarrow D_s^{*+} D_s^-$	< 1.3 [BaBar][24]	$0.25^{+0.08+0.06+0.01}_{-0.08-0.08-0.01}$	$\sim -10^{-3}$	
9 $\bar{B}_s^0 \rightarrow D^{*0} \bar{D}^0$		$4.3^{+1.3+0.8+0.1}_{-1.3-1.1-0.2}$	$0.2^{+0.0+0.0}_{-0.1-0.1}$	
10 $\bar{B}_s^0 \rightarrow D^{*+} D^-$		$4.4^{+1.4+0.9+0.1}_{-1.3-1.2-0.2}$...	

TABLE IV: CP averaging branching ratios for $B \rightarrow VV$ (unit: 10^{-4}) and the ratios of the transverse polarizations' contribution.

Channels	\mathcal{BR}		\mathcal{R}_T	
	Exp.	This work	Exp.	This work
1 $B^- \rightarrow D^{*0} D^{*-}$	$8.1 \pm 1.2 \pm 1.2$ [Babar][25]	$6.8^{+5.0+1.5+0.1}_{-3.2-2.0-0.4}$		$0.45^{+0.13}_{-0.13}$
2 $B^- \rightarrow D^{*0} D_s^{*-}$	175 ± 23	$181^{+139+41+3.5}_{-95-53-10}$		$0.48^{+0.12}_{-0.14}$
3 $\bar{B}^0 \rightarrow D^{*+} D^{*-}$	8.2 ± 0.9	$6.3^{+4.8+1.1+0.1}_{-3.0-1.6-0.4}$	$0.43 \pm 0.08 \pm 0.02$	$0.46^{+0.14}_{-0.14}$
4 $\bar{B}^0 \rightarrow D^{*+} D_s^{*-}$	179 ± 14	$168^{+130+39+3.2}_{-88-48-9.6}$	0.48 ± 0.05	$0.48^{+0.13}_{-0.14}$
5 $\bar{B}_s^0 \rightarrow D_s^{*+} D^{*-}$		$3.9^{+2.6+1.2+0.1}_{-1.9-1.3-0.2}$		$0.44^{+0.14}_{-0.14}$
6 $\bar{B}_s^0 \rightarrow D_s^{*+} D_s^{*-}$		$99^{+72+26+1.9}_{-54-29-5.6}$		$0.47^{+0.15}_{-0.15}$
7 $\bar{B}^0 \rightarrow D^{*0} \bar{D}^{*0}$	< 0.9 [Babar][25]	$0.15^{+0.05+0.03+0.00}_{-0.04-0.03-0.01}$		$0.47^{+0.35}_{-0.29}$
8 $\bar{B}^0 \rightarrow D_s^{*+} D_s^{*-}$	< 2.4 [Babar][24]	$0.19^{+0.10+0.06+0.00}_{-0.07-0.05-0.01}$		$0.57^{+0.33}_{-0.37}$
9 $\bar{B}_s^0 \rightarrow D^{*0} \bar{D}^{*0}$		$2.8^{+1.1+0.7+0.1}_{-0.8-0.6-0.2}$		$0.48^{+0.37}_{-0.27}$
10 $\bar{B}_s^0 \rightarrow D^{*+} D^{*-}$		$3.1^{+1.0+0.9+0.1}_{-0.8-0.7-0.2}$		$0.49^{+0.34}_{-0.29}$

1. In each table the channels 1 and 3 should have similar branching ratios because they have the same CKM matrix elements for the factorizable emission diagrams and similar transition form factors for isospin symmetry. For the same reason, channels 2 and 4 should also have similar branching ratios.
2. The branching ratios of channels 4 and 6 indicate that the $\bar{B}_s \rightarrow D_s^{(*)}$ transition has a little smaller form factor than $B \rightarrow D^{(*)}$ transition. The reason is that the antistrange quark in the \bar{B}_s meson has a little larger momentum fraction than the d quark in the \bar{B}^0 meson due to the SU(3) breaking effect [28]. In [29], the

TABLE V: CP asymmetry and the ratios of P-wave contributions in branching ratios for $B \rightarrow VV$ decays.

Channels	$A_{CP}^{\text{dir}}(\%)$		A_{CP}^{mix}		R_{\perp}
	Exp.	This work	Exp.	This work	
1 $B^- \rightarrow D^{*0} D^{*-}$		$0.2^{+0.0+0.0}_{-0.1-0.1}$...	0.17
2 $B^- \rightarrow D^{*0} D_s^{*-}$		$\sim -10^{-3}$...	0.16
3 $\bar{B}^0 \rightarrow D^{*+} D^{*-}$	2 ± 10	$\sim -10^{-2}$	-0.67 ± 0.18	$-0.76^{+0.00+0.03+0.02}_{-0.01-0.03-0.02}$	0.16
4 $\bar{B}^0 \rightarrow D^{*+} D_s^{*-}$		
5 $\bar{B}_s^0 \rightarrow D_s^{*+} D^{*-}$		$0.1^{+0.1+0.1}_{-0.0-0.0}$...	0.14
6 $\bar{B}_s^0 \rightarrow D_s^{*+} D_s^{*-}$		0.17
7 $\bar{B}^0 \rightarrow D^{*0} \bar{D}^{*0}$		$-3.4^{+0.4+0.4}_{-0.5-1.8}$		$-0.73^{+0.03+0.23+0.01}_{-0.05-0.14-0.01}$	0.24
8 $\bar{B}^0 \rightarrow D_s^{*+} D_s^{*-}$		$-0.4^{+0.1+0.3}_{-0.1-0.2}$		$-0.68^{+0.03+0.27+0.01}_{-0.06-0.17-0.01}$	0.32
9 $\bar{B}_s^0 \rightarrow D^{*0} \bar{D}^{*0}$		$0.2^{+0.0+0.0}_{-0.1-0.0}$		$\sim 10^{-3}$	0.25
10 $\bar{B}_s^0 \rightarrow D^{*+} D^{*-}$		0.29

$\bar{B}_s \rightarrow D_s$ transition is investigated with the light-cone sum rules, and a similar branching ratio for $\bar{B}_s \rightarrow D_s^+ D_s^-$ is obtained under the factorization assumption. This means the PQCD and the light-cone sum rules have the similar $\bar{B}_s \rightarrow D_s$ transition form factors.

- The first 6 $B \rightarrow PP$ decays in Table I and the corresponding 6 $B \rightarrow PV$ decays in Table II have the same transition form factors, respectively, as well as the similar decay constants between D meson and D^* meson. Thus their branching ratios should also be similar. However, such phenomena are not expected in $B \rightarrow VP$ decays and $B \rightarrow VV$ decays, because in addition to the longitudinal polarization's contributions, the $B \rightarrow VV$ decays also receive large contributions from transverse polarizations.

From Tables I, II, III, and IV, one can find that most experimental branching ratios agree with our conclusions in the above paragraphs very well within the errors. The authors in Refs. [26, 27] also investigate the decays of B to double charmed mesons under factorization assumption, but with different models. Their results also indicate that the factorization works well.

Since the direct CP asymmetry is proportional to the interference between the tree and penguin contributions [10], it should be small because of the small penguin contributions as we mentioned above. Our numerical results indeed indicate that the direct CP violations are very small. A relatively large direct CP violation appears in the pure annihilation decay $\bar{B}^0 \rightarrow D^0 \bar{D}^0$ and its corresponding $B \rightarrow PV$, VP , and VV decays. However it is still only several percent. Although the experiments give somehow large direct CP asymmetry in some channels, the uncertainty is still large. Any large direct CP violation observed in experiments would be treated as a signal of new physics at first.

The mixing induced CP asymmetry in B decays is almost proportional to the $\sin 2\beta$ from Eq.(53), if we neglect the small contribution from penguin contributions. It should be mentioned that, experimentally the P wave component in the amplitudes of $B \rightarrow VV$ mode will bring systematic errors in the results of mixing induced CP asymmetry

because they will bring a minus sign relative to the S and D wave component. Our results for A_{CP}^{mix} in Table V only include the S wave and D wave contributions, and in this table we also give the values of R_{\perp} , which is defined by the ratio of branching fractions with only P wave component and that with all the contributions. Because the P wave contributions are very small in the color allowed tree dominated processes, the experimental measurements are still in agreement with our calculations. For the pure annihilation processes, the P-wave contributions are relatively large and therefore these channels may not be good choices for the observation of mixing induced CP asymmetry.

In Table IV, we give the ratios of transverse polarizations' contributions in branching ratios. One can find that both in the processes with an external W emission and in the pure annihilation decays, the transverse polarizations take about 40% – 50% of the contributions, which agree with the present experimental data amazingly well. We should point out that these ratios are very sensitive to the terms with power r^2 ($r = m_D/m_B$), although these corrections change the other observables only a little. With the r^2 corrections absent, the ratios of transverse polarizations for the channels with an external W emission are about 20%, and those for the pure annihilation channels are 0, because the transverse polarization's contributions for these channels are at the power of r^2 . For the sensitivity of these ratios to the power correction terms, we vary the variable r by 20% for an error estimation in Table IV. In [30], the authors obtain the values for the ratios $\sim 50\%$ for the external W emission processes simply by means of kinematics under the naive factorization, which agree with our results. For the pure annihilation decays, the transverse polarizations are suppressed by r^2 , which is the reason why the authors in [30] think the ratios of the transverse polarizations are very small. However, our calculation show that, with the r^2 terms included, these ratios increase to about 50%. This means that the polarization fractions are quite sensitive to the power corrections although they are not sensitive to the higher order QCD corrections etc. The future experiments will tell us more about the polarizations in the pure annihilation processes.

IV. SUMMARY

Although the D meson mass is not very small compared with the B meson mass, factorization can still work in the leading order of m_D/m_B and Λ_{QCD}/m_D expansion. Since the PQCD approach can eliminate the end-point singularity in the perturbative calculation, we investigate the decays of B to double charmed mesons systematically. Both pseudoscalar and vector charmed mesons are included in the final states. We find that the factorizable emission diagrams are dominant in the branching ratios. Most of our branching ratios agree with the experimental data, which means the factorization assumption works well. However, experimental data show that there are still some discrepancies, which means more work is needed both at the theoretical side and the experimental side.

Our results indicate that the direct CP asymmetries in these channels are very small. Thus, it will be a signal of new physics if a large direct CP asymmetry appears. In the decays of B to double vector charmed mesons, the transverse polarizations contribute 40% – 50% both in the external W emission processes and in the pure annihilation decays, which agree with the present experimental data. We should mention that the correction terms at the power of r^2 play an important role in transverse polarizations, without which the ratios for the external W emission processes decrease to about 20% and for the pure annihilation decays the ratios are 0 because of the r^2 suppression.

V. ACKNOWLEDGEMENT

This work is partly supported by National Natural Science Foundation of China under Grants No. 10735080, No. 10625525, and No. 10525523. We would like to thank W. Wang, Y.M. Wang, H. Zou, K. Ukai and A.Satpath for valuable discussions.

Appendix A: scales and functions for the hard kernel

The variables that are used to determine the scales and the expressions of the hard kernels are defined by

$$\begin{aligned}
P_{en} &= m_B^2 x_1 x_2 (1 - r_3^2), \\
P_{en}^{(1)} &= m_B^2 x_2 (x_1 (1 - r_3^2) - x_3 (1 - r_2^2 - r_3^2)), \\
P_{en}^{(2)} &= -m_B^2 [x_2 (x_3 - 1) r_2^2 + r_3^2 (x_1 (x_2 - 1) + x_2 (x_3 - 1) - x_3) - x_2 (x_1 + x_3 - 1)], \\
P_{an} &= m_B^2 (1 - (1 - r_2^2) x_3 - x_2 (1 - x_3 (1 - r_2^2) - (1 - x_3) r_3^2)), \\
P_{an}^{(1)} &= m_B^2 (1 + x_1 x_2 (1 - r_3^2) - (1 - r_2^2 - r_3^2) x_2 x_3), \\
P_{an}^{(2)} &= m_B^2 (-x_3 r_2^2 + x_1 ((r_3^2 - 1) x_2 + 1) + x_3 + x_2 ((x_3 - 1) r_3^2 + (r_2^2 - 1) x_3 + 1) - 1), \\
P_{an}^{(c)} &= m_B^2 (1 - r_2^2 - r_3^2) x_2 x_3, \\
P_{an}^{(1c)} &= m_B^2 [x_1 ((r_3^2 - 1) x_2 + 1) - (r_2^2 - 1) x_3 + x_2 ((x_3 - 1) r_3^2 + (r_2^2 - 1) x_3 + 1)], \\
P_{an}^{(2c)} &= m_B^2 x_2 ((r_2^2 + r_3^2 - 1) x_3 - (r_3^2 - 1) x_1).
\end{aligned} \tag{A1}$$

The scales are determined as

$$\begin{aligned}
t_e^{(1)} &= \max\{\sqrt{x_2 (1 - r_3^2)} m_B f_{\text{err}}, 1/b_1, 1/b_2\}, \\
t_e^{(2)} &= \max\{\sqrt{x_1 (1 - r_3^2)} m_B f_{\text{err}}, 1/b_1, 1/b_2\}, \\
t_{en}^{(1)} &= \max\{\sqrt{|P_{en}|} f_{\text{err}}, \sqrt{|P_{en}^{(1)}|} f_{\text{err}}, 1/b_1, 1/b_3\}, \\
t_{en}^{(2)} &= \max\{\sqrt{|P_{en}|} f_{\text{err}}, \sqrt{|P_{en}^{(2)}|} f_{\text{err}}, 1/b_1, 1/b_3\}, \\
t_a^{(1)} &= \max\{\sqrt{1 - (1 - r_3^2) x_2} m_B f_{\text{err}}, 1/b_2, 1/b_3\}, \\
t_a^{(2)} &= \max\{\sqrt{1 - (1 - r_2^2) x_3} m_B f_{\text{err}}, 1/b_2, 1/b_3\}, \\
t_{an}^{(1)} &= \max\{\sqrt{|P_{an}|} f_{\text{err}}, \sqrt{|P_{an}^{(1)}|} f_{\text{err}}, 1/b_1, 1/b_2\}, \\
t_{an}^{(2)} &= \max\{\sqrt{|P_{an}|} f_{\text{err}}, \sqrt{|P_{an}^{(2)}|} f_{\text{err}}, 1/b_1, 1/b_2\}, \\
t_a^{(1c)} &= \max\{\sqrt{(1 - r_2^2 - r_3^2) x_3} m_B f_{\text{err}}, 1/b_2, 1/b_3\}, \\
t_a^{(2c)} &= \max\{\sqrt{(1 - r_2^2 - r_3^2) x_2} m_B f_{\text{err}}, 1/b_2, 1/b_3\}, \\
t_{an}^{(1c)} &= \max\{\sqrt{|P_{an}^{(c)}|} f_{\text{err}}, \sqrt{|P_{an}^{(1c)}|} f_{\text{err}}, 1/b_1, 1/b_2\}, \\
t_{an}^{(2c)} &= \max\{\sqrt{|P_{an}^{(c)}|} f_{\text{err}}, \sqrt{|P_{an}^{(2c)}|} f_{\text{err}}, 1/b_1, 1/b_2\},
\end{aligned} \tag{A2}$$

with f_{err} varies from 0.75 to 1.25 for an error estimation.

The functions of the hard kernels that appear in the factorization formulae are given by

$$\begin{aligned}
h_e(x_1, x_2, b_1, b_2) &= K_0(\sqrt{x_1 x_2} m_B b_1) \\
&\times [\theta(b_1 - b_2) K_0(\sqrt{x_2} m_B b_1) I_0(\sqrt{x_2} m_B b_2) \\
&+ \theta(b_2 - b_1) K_0(\sqrt{x_2} m_B b_2) I_0(\sqrt{x_2} m_B b_1)] , \\
h_a(x_2, x_3, b_2, b_3) &= \left(i\frac{\pi}{2}\right)^2 H_0^{(1)}(\sqrt{x_2 x_3} m_B b_2) \\
&\times \left[\theta(b_2 - b_3) H_0^{(1)}(\sqrt{x_3} m_B b_2) J_0(\sqrt{x_3} m_B b_3) \right. \\
&\left. + \theta(b_3 - b_2) H_0^{(1)}(\sqrt{x_3} m_B b_3) J_0(\sqrt{x_3} m_B b_2) \right] , \\
h_{en}^{(j)} &= \left[\theta(b_1 - b_3) K_0(\sqrt{P_{en}} b_1) I_0(\sqrt{P_{en}} b_3) + \theta(b_3 - b_1) K_0(\sqrt{P_{en}} b_3) I_0(\sqrt{P_{en}} b_1) \right] \\
&\times \left\{ \begin{array}{l} K_0(\sqrt{|P_{en}^{(j)}|} b_3) \quad \text{for } P_{en}^{(j)} \geq 0 \\ \frac{i\pi}{2} H_0^{(1)}(\sqrt{|P_{en}^{(j)}|} b_3) \quad \text{for } P_{en}^{(j)} \leq 0 \end{array} \right\} , \\
h_{an}^{(j)} &= i\frac{\pi}{2} \left[\theta(b_1 - b_2) H_0^{(1)}(\sqrt{P_{an}} b_1) J_0(\sqrt{P_{an}} b_2) + \theta(b_2 - b_1) H_0^{(1)}(\sqrt{P_{an}} b_2) J_0(\sqrt{P_{an}} b_1) \right] \\
&\times \left\{ \begin{array}{l} K_0(\sqrt{|P_{an}^{(j)}|} b_1) \quad \text{for } P_{an}^{(j)} \geq 0 \\ \frac{i\pi}{2} H_0^{(1)}(\sqrt{|P_{an}^{(j)}|} b_1) \quad \text{for } P_{an}^{(j)} \leq 0 \end{array} \right\} , \tag{A3}
\end{aligned}$$

and the functions that consist of coupling constant and Sudakov factors are given by

$$\begin{aligned}
E_e(t) &= \alpha_s(t) \exp[-S_B(t) - S_{M_2}(t)] , \\
E_a(t) &= \alpha_s(t) \exp[-S_{M_2}(t) - S_{M_3}(t)] , \\
E_{en}(t) &= \alpha_s(t) \exp[-S_B(t) - S_{M_2} - S_{M_3}|_{b_2=b_1}] , \\
E_{an}(t) &= \alpha_s(t) \exp[-S_B(t) - S_{M_2} - S_{M_3}|_{b_3=b_2}] , \tag{A4}
\end{aligned}$$

where

$$S_B(t) = S_{M_2} = S_{M_3} = s\left(x_1 \frac{m_B}{\sqrt{2}}, b_1\right) + \frac{5}{3} \int_{1/b_1}^t \frac{d\bar{\mu}}{\bar{\mu}} \gamma_q(\alpha_s(\bar{\mu})) , \tag{A5}$$

with the quark anomalous dimension $\gamma_q = -\alpha_s/\pi$. The explicit form for the function $s(Q, b)$ is:

$$\begin{aligned}
s(Q, b) &= \frac{A^{(1)}}{2\beta_1} \hat{q} \ln\left(\frac{\hat{q}}{\hat{b}}\right) - \frac{A^{(1)}}{2\beta_1} (\hat{q} - \hat{b}) + \frac{A^{(2)}}{4\beta_1^2} \left(\frac{\hat{q}}{\hat{b}} - 1\right) - \left[\frac{A^{(2)}}{4\beta_1^2} - \frac{A^{(1)}}{4\beta_1} \ln\left(\frac{e^{2\gamma_E - 1}}{2}\right)\right] \ln\left(\frac{\hat{q}}{\hat{b}}\right) \\
&+ \frac{A^{(1)}\beta_2}{4\beta_1^3} \hat{q} \left[\frac{\ln(2\hat{q}) + 1}{\hat{q}} - \frac{\ln(2\hat{b}) + 1}{\hat{b}} \right] + \frac{A^{(1)}\beta_2}{8\beta_1^3} [\ln^2(2\hat{q}) - \ln^2(2\hat{b})] , \tag{A6}
\end{aligned}$$

where the variables are defined by

$$\hat{q} \equiv \ln[Q/(\sqrt{2}\Lambda)] , \quad \hat{b} \equiv \ln[1/(b\Lambda)] , \tag{A7}$$

and the coefficients $A^{(i)}$ and β_i are

$$\begin{aligned}
\beta_1 &= \frac{33 - 2n_f}{12} , \quad \beta_2 = \frac{153 - 19n_f}{24} , \\
A^{(1)} &= \frac{4}{3} , \quad A^{(2)} = \frac{67}{9} - \frac{\pi^2}{3} - \frac{10}{27} n_f + \frac{8}{3} \beta_1 \ln\left(\frac{1}{2} e^{\gamma_E}\right) , \tag{A8}
\end{aligned}$$

n_f is the number of the quark flavors and γ_E is the Euler constant. We will use the one-loop running coupling constant, i.e. we pick up the four terms in the first line of the expression for the function $s(Q, b)$.

Appendix B: factorization formulae for $B \rightarrow PV$ (M_2 is a pseudoscalar meson and M_3 is a vector meson)

$$\begin{aligned}
F_e^{LL}(a_i(t)) &= 8\pi C_F f_{M_3} m_B^4 \int_0^1 dx_1 dx_2 \int_0^{1/\Lambda} b_1 db_1 b_2 db_2 \phi_B(x_1, b_1) \phi_{M_2}(x_2) \\
&\quad \times \left[-((2x_2 - 1)r_2 - x_2 - 1) E_e(t_e^{(1)}) a_i(t_e^{(1)}) h_e(x_1, x_2(1 - r_3^2), b_1, b_2) S_t(x_2) \right. \\
&\quad \left. + r_2(1 + r_2) E_e(t_e^{(2)}) a_i(t_e^{(2)}) h_e(x_2, x_1(1 - r_3^2), b_2, b_1) S_t(x_1) \right], \tag{B1}
\end{aligned}$$

$$F_e^{SP}(a_i(t)) = 0, \tag{B2}$$

$$\begin{aligned}
F_{en}^{LL}(a_i(t)) &= 16\pi \sqrt{\frac{2}{3}} C_F m_B^4 \int_0^1 [dx] \int_0^{1/\Lambda} b_1 db_1 b_3 db_3 \phi_B(x_1, b_1) \phi_{M_2}(x_2) \phi_{M_3}(x_3) \\
&\quad \times \left[(-x_2 r_2 + x_3) E_b(t_{en}^{(1)}) a_i(t_{en}^{(1)}) h_{en}^{(1)}(x_i, b_i) \right. \\
&\quad \left. + (x_2 r_2 - x_2 + x_3 - 1) E_{en}(t_{en}^{(2)}) a_i(t_{en}^{(2)}) h_{en}^{(2)}(x_i, b_i) \right], \tag{B3}
\end{aligned}$$

$$\begin{aligned}
F_{en}^{LR}(a_i(t)) &= 16\pi \sqrt{\frac{2}{3}} C_F m_B^4 \int_0^1 [dx] \int_0^{1/\Lambda} b_1 db_1 b_3 db_3 \phi_B(x_1, b_1) \phi_{M_2}(x_2) \phi_{M_3}(x_3) \\
&\quad \times r_3 \left[(x_3 - r_2(x_2 - x_3)) E_{en}(t_{en}^{(1)}) a_i(t_{en}^{(1)}) h_{en}^{(1)}(x_i, b_i) \right. \\
&\quad \left. - (x_3 + r_2(x_2 + x_3)) E_{en}(t_{en}^{(2)}) a_i(t_{en}^{(2)}) h_{en}^{(2)}(x_i, b_i) \right], \tag{B4}
\end{aligned}$$

$$\begin{aligned}
F_a^{LL}(a_i(t)) &= 8\pi C_F f_B m_B^4 \int_0^1 dx_2 dx_3 \int_0^{1/\Lambda} b_2 db_2 b_3 db_3 \phi_{M_2}(x_2) \phi_{M_3}(x_3) \\
&\quad \times \left[(x_2 - 1) E_a(t_a^{(1)}) a_i(t_a^{(1)}) h_a(1 - (1 - r_2^2)x_3, 1 - (1 - r_3^2)x_2, b_3, b_2) S_t(x_2) \right. \\
&\quad \left. + (-2r_2 r_3 x_3 - (x_3 - 1)) E_a(t_a^{(2)}) a_i(t_a^{(2)}) h_a(1 - (1 - r_3^2)x_2, 1 - (1 - r_2^2)x_3, b_2, b_3) S_t(x_3) \right], \tag{B5}
\end{aligned}$$

$$F_a^{LR}(a_i(t)) = -F_a^{LL}(a_i(t)), \tag{B6}$$

$$\begin{aligned}
F_a^{SP}(a_i(t)) &= 16\pi C_F f_B m_B^4 \int_0^1 dx_2 dx_3 \int_0^{1/\Lambda} b_2 db_2 b_3 db_3 \phi_{M_2}(x_2) \phi_{M_3}(x_3) \\
&\quad \times \left[r_2(1 - x_2) E_a(t_a^{(1)}) a_i(t_a^{(1)}) h_a(1 - (1 - r_2^2)x_3, 1 - (1 - r_3^2)x_2, b_3, b_2) S_t(x_2) \right. \\
&\quad \left. + (2r_2 + r_3(x_3 - 1)) E_a(t_a^{(2)}) a_i(t_a^{(2)}) h_a(1 - (1 - r_3^2)x_2, 1 - (1 - r_2^2)x_3, b_2, b_3) S_t(x_3) \right], \tag{B7}
\end{aligned}$$

$$\begin{aligned}
F_{ac}^{LL}(a_i(t)) &= 8\pi C_F f_B m_B^4 \int_0^1 dx_2 dx_3 \int_0^{1/\Lambda} b_2 db_2 b_3 db_3 \phi_{M_2}(x_2) \phi_{M_3}(x_3) \\
&\quad \times \left[(r_2 r_3(1 - 2x_3) - x_3) E_a(t_a^{(1c)}) a_i(t_a^{(1c)}) h_a(x_2, x_3(1 - r_2^2 - r_3^2), b_2, b_3) S_t(x_3) \right. \\
&\quad \left. + (r_2 r_3 + x_2) E_a(t_a^{(2c)}) a_i(t_a^{(2c)}) h_a(x_3, x_2(1 - r_2^2 - r_3^2), b_3, b_2) S_t(x_2) \right], \tag{B8}
\end{aligned}$$

$$F_{ac}^{LR}(a_i(t)) = -F_{ac}^{LL}(a_i(t)), \tag{B9}$$

$$\begin{aligned}
F_{an}^{LL}(a_i(t)) &= 16\pi \sqrt{\frac{2}{3}} C_F m_B^4 \int_0^1 [dx] \int_0^{1/\Lambda} b_1 db_1 b_2 db_2 \phi_B(x_1, b_1) \phi_{M_2}(x_2) \phi_{M_3}(x_3) \\
&\quad \times \left[(r_2 r_3(x_3 - x_2) + x_3 - 1) E_{an}(t_{an}^{(1)}) a_i(t_{an}^{(1)}) h_{an}^{(1)}(x_i, b_i) \right. \\
&\quad \left. + (r_2 r_3(x_3 - x_2) - x_2 + 1) E_{an}(t_{an}^{(2)}) a_i(t_{an}^{(2)}) h_{an}^{(2)}(x_i, b_i) \right], \tag{B10}
\end{aligned}$$

$$\begin{aligned}
F_{an}^{LR}(a_i(t)) &= 16\pi\sqrt{\frac{2}{3}}C_F m_B^4 \int_0^1 [dx] \int_0^{1/\Lambda} b_1 db_1 b_2 db_2 \phi_B(x_1, b_1) \phi_{M_2}(x_2) \phi_{M_3}(x_3) \\
&\times \left[-(r_2(x_2 + 1) - r_3(x_3 + 1)) E_{an}(t_{an}^{(1)}) a_i(t_{an}^{(1)}) h_{an}^{(1)}(x_i, b_i) \right. \\
&\left. + (r_2(x_2 - 1) - r_3(x_3 - 1)) E_{an}(t_{an}^{(2)}) a_i(t_{an}^{(2)}) h_{an}^{(2)}(x_i, b_i) \right], \tag{B11}
\end{aligned}$$

$$\begin{aligned}
F_{an}^{SP}(a_i(t)) &= 16\pi\sqrt{\frac{2}{3}}C_F m_B^4 \int_0^1 [dx] \int_0^{1/\Lambda} b_1 db_1 b_2 db_2 \phi_B(x_1, b_1) \phi_{M_2}(x_2) \phi_{M_3}(x_3) \\
&\times \left[-(r_2 r_3(x_2 - x_3) + x_2 - 1) E_{an}(t_{an}^{(1)}) a_i(t_{an}^{(1)}) h_{an}^{(1)}(x_i, b_i) \right. \\
&\left. - (r_2 r_3(x_2 - x_3) - x_3 + 1) E_{an}(t_{an}^{(2)}) a_i(t_{an}^{(2)}) h_{an}^{(2)}(x_i, b_i) \right], \tag{B12}
\end{aligned}$$

$$\begin{aligned}
F_{anc}^{LL}(a_i(t)) &= 16\pi\sqrt{\frac{2}{3}}C_F m_B^4 \int_0^1 [dx] \int_0^{1/\Lambda} b_1 db_1 b_2 db_2 \phi_B(x_1, b_1) \phi_{M_2}(x_2) \phi_{M_3}(x_3) \\
&\times \left[(r_2 r_3(x_3 - x_2) - x_2) E_{an}(t_{an}^{(1c)}) a_i(t_{an}^{(1c)}) h_{an}^{(1c)}(x_i, b_i) \right. \\
&\left. + (r_2 r_3(x_3 - x_2) + x_3) E_{an}(t_{an}^{(2c)}) a_i(t_{an}^{(2c)}) h_{an}^{(2c)}(x_i, b_i) \right], \tag{B13}
\end{aligned}$$

$$\begin{aligned}
F_{anc}^{SP}(a_i(t)) &= 16\pi\sqrt{\frac{2}{3}}C_F m_B^4 \int_0^1 [dx] \int_0^{1/\Lambda} b_1 db_1 b_2 db_2 \phi_B(x_1, b_1) \phi_{M_2}(x_2) \phi_{M_3}(x_3) \\
&\times \left[(r_2 r_3(x_3 - x_2) + x_3) E_{an}(t_{an}^{(1c)}) a_i(t_{an}^{(1c)}) h_{an}^{(1c)}(x_i, b_i) \right. \\
&\left. - ((r_2 r_3 + 1)x_2 - r_3 x_3 (r_2 + r_3)) E_{an}(t_{an}^{(2c)}) a_i(t_{an}^{(2c)}) h_{an}^{(2c)}(x_i, b_i) \right], \tag{B14}
\end{aligned}$$

Appendix C: factorization formulae for $B \rightarrow VP$ (M_2 is a vector meson and M_3 is a pseudoscalar meson)

$$\begin{aligned}
F_e^{LL}(a_i(t)) &= 8\pi C_F f_{M_3} m_B^4 \int_0^1 dx_1 dx_2 \int_0^{1/\Lambda} b_1 db_1 b_2 db_2 \phi_B(x_1, b_1) \phi_{M_2}(x_2) \\
&\times \left[-((2x_2 - 1)r_2 - x_2 - 1) E_e(t_e^{(1)}) a_i(t_e^{(1)}) h_e(x_1, x_2(1 - r_3^2), b_1, b_2) S_t(x_2) \right. \\
&\left. + r_2(1 + r_2) E_e(t_e^{(2)}) a_i(t_e^{(2)}) h_e(x_2, x_1(1 - r_3^2), b_2, b_1) S_t(x_1) \right], \tag{C1}
\end{aligned}$$

$$\begin{aligned}
F_e^{SP}(a_i(t)) &= 16\pi C_F f_{M_3} m_B^4 \int_0^1 dx_1 dx_2 \int_0^{1/\Lambda} b_1 db_1 b_2 db_2 \phi_B(x_1, b_1) \phi_{M_2}(x_2) \\
&\times r_3 \left[(r_2 x_2 - 1) E_e(t_e^{(1)}) a_i(t_e^{(1)}) h_e(x_1, x_2(1 - r_3^2), b_1, b_2) S_t(x_2) \right. \\
&\left. - r_2 E_e(t_e^{(2)}) a_i(t_e^{(2)}) h_e(x_2, x_1(1 - r_3^2), b_2, b_1) S_t(x_1) \right], \tag{C2}
\end{aligned}$$

$$\begin{aligned}
F_{en}^{LL}(a_i(t)) &= 16\pi\sqrt{\frac{2}{3}}C_F m_B^4 \int_0^1 [dx] \int_0^{1/\Lambda} b_1 db_1 b_3 db_3 \phi_B(x_1, b_1) \phi_{M_2}(x_2) \phi_{M_3}(x_3) \\
&\times \left[-(-x_2 r_2 - x_3) E_{en}(t_{en}^{(1)}) a_i(t_{en}^{(1)}) h_{en}^{(1)}(x_i, b_i) \right. \\
&\left. + (x_2 r_2 - x_2 + x_3 - 1) E_{en}(t_{en}^{(2)}) a_i(t_{en}^{(2)}) h_{en}^{(2)}(x_i, b_i) \right], \tag{C3}
\end{aligned}$$

$$\begin{aligned}
F_{en}^{LR}(a_i(t)) &= 16\pi\sqrt{\frac{2}{3}}C_F m_B^4 \int_0^1 [dx] \int_0^{1/\Lambda} b_1 db_1 b_3 db_3 \phi_B(x_1, b_1) \phi_{M_2}(x_2) \phi_{M_3}(x_3) \\
&\quad \times r_3 \left[-(r_2(x_2 - x_3) + x_3) E_{en}(t_{en}^{(1)}) a_i(t_{en}^{(1)}) h_{en}^{(1)}(x_i, b_i) \right. \\
&\quad \left. + (r_2(x_2 + x_3 - 2) - x_3 + 2) E_{en}(t_{en}^{(2)}) a_i(t_{en}^{(2)}) h_{en}^{(2)}(x_i, b_i) \right], \tag{C4}
\end{aligned}$$

$$\begin{aligned}
F_a^{LL}(a_i(t)) &= 8\pi C_F f_B m_B^4 \int_0^1 dx_2 dx_3 \int_0^{1/\Lambda} b_2 db_2 b_3 db_3 \phi_{M_2}(x_2) \phi_{M_3}(x_3) \\
&\quad \times [(2r_2 r_3 x_2 + x_2 - 1) \\
&\quad \times E_a(t_a^{(1)}) a_i(t_a^{(1)}) h_a(1 - (1 - r_2^2)x_3, 1 - (1 - r_3^2)x_2, b_3, b_2) S_t(x_2) \\
&\quad + (1 - x_3) E_a(t_a^{(2)}) a_i(t_a^{(2)}) h_a(1 - (1 - r_3^2)x_2, 1 - (1 - r_2^2)x_3, b_2, b_3) S_t(x_3)] , \tag{C5}
\end{aligned}$$

$$F_a^{LR}(a_i(t)) = -F_a^{LL}(a_i(t)), \tag{C6}$$

$$\begin{aligned}
F_a^{SP}(a_i(t)) &= 16\pi C_F f_B m_B^4 \int_0^1 dx_2 dx_3 \int_0^{1/\Lambda} b_2 db_2 b_3 db_3 \phi_{M_2}(x_2) \phi_{M_3}(x_3) \\
&\quad \times \left[-(2r_3 + r_2(x_2 - 1)) E_a(t_a^{(1)}) a_i(t_a^{(1)}) h_a(1 - (1 - r_2^2)x_3, 1 - (1 - r_3^2)x_2, b_3, b_2) S_t(x_2) \right. \\
&\quad \left. + r_3(x_3 - 1) E_a(t_a^{(2)}) a_i(t_a^{(2)}) h_a(1 - (1 - r_3^2)x_2, 1 - (1 - r_2^2)x_3, b_2, b_3) S_t(x_3) \right], \tag{C7}
\end{aligned}$$

$$\begin{aligned}
F_{ac}^{LL}(a_i(t)) &= 8\pi C_F f_B m_B^4 \int_0^1 dx_2 dx_3 \int_0^{1/\Lambda} b_2 db_2 b_3 db_3 \phi_{M_2}(x_2) \phi_{M_3}(x_3) \\
&\quad \times \left[(-r_2 r_3 - x_3) E_a(t_a^{(1c)}) a_i(t_a^{(1c)}) h_a(x_2, x_3(1 - r_2^2 - r_3^2), b_2, b_3) S_t(x_3) \right. \\
&\quad \left. - (r_2 r_3(1 - 2x_2) - x_2) a_i(t_a^{(2c)}) h_a(x_3, x_2(1 - r_2^2 - r_3^2), b_3, b_2) S_t(x_2) \right], \tag{C8}
\end{aligned}$$

$$F_{ac}^{LR}(a_i(t)) = -F_{ac}^{LL}(a_i(t)), \tag{C9}$$

$$\begin{aligned}
F_{an}^{LL}(a_i(t)) &= 16\pi\sqrt{\frac{2}{3}}C_F m_B^4 \int_0^1 [dx] \int_0^{1/\Lambda} b_1 db_1 b_2 db_2 \phi_B(x_1, b_1) \phi_{M_2}(x_2) \phi_{M_3}(x_3) \\
&\quad \times \left[-(r_2 r_3(x_2 - x_3) - x_3 + 1) E_{an}(t_{an}^{(1)}) a_i(t_{an}^{(1)}) h_{an}^{(1)}(x_i, b_i) \right. \\
&\quad \left. + (r_2 r_3(x_3 - x_2) - x_2 + 1) E_{an}(t_{an}^{(2)}) a_i(t_{an}^{(2)}) h_{an}^{(2)}(x_i, b_i) \right], \tag{C10}
\end{aligned}$$

$$\begin{aligned}
F_{an}^{LR}(a_i(t)) &= 16\pi\sqrt{\frac{2}{3}}C_F m_B^4 \int_0^1 [dx] \int_0^{1/\Lambda} b_1 db_1 b_2 db_2 \phi_B(x_1, b_1) \phi_{M_2}(x_2) \phi_{M_3}(x_3) \\
&\quad \times \left[(r_2(x_2 + 1) - r_3(x_3 + 1)) E_{an}(t_{an}^{(1)}) a_i(t_{an}^{(1)}) h_{an}^{(1)}(x_i, b_i) \right. \\
&\quad \left. - (r_2(x_2 - 1) - r_3(x_3 - 1)) E_{an}(t_{an}^{(2)}) a_i(t_{an}^{(2)}) h_{an}^{(2)}(x_i, b_i) \right], \tag{C11}
\end{aligned}$$

$$\begin{aligned}
F_{an}^{SP}(a_i(t)) &= 16\pi\sqrt{\frac{2}{3}}C_F m_B^4 \int_0^1 [dx] \int_0^{1/\Lambda} b_1 db_1 b_2 db_2 \phi_B(x_1, b_1) \phi_{M_2}(x_2) \phi_{M_3}(x_3) \\
&\quad \times \left[(r_2 r_3(x_3 - x_2) - x_2 + 1) E_{an}(t_{an}^{(1)}) a_i(t_{an}^{(1)}) h_{an}^{(1)}(x_i, b_i) \right. \\
&\quad \left. - (r_2 r_3(x_2 - x_3) - x_3 + 1) E_{an}(t_{an}^{(2)}) a_i(t_{an}^{(2)}) h_{an}^{(2)}(x_i, b_i) \right], \tag{C12}
\end{aligned}$$

$$\begin{aligned}
F_{anc}^{LL}(a_i(t)) &= 16\pi\sqrt{\frac{2}{3}}C_F m_B^4 \int_0^1 [dx] \int_0^{1/\Lambda} b_1 db_1 b_2 db_2 \phi_B(x_1, b_1) \phi_{M_2}(x_2) \phi_{M_3}(x_3) \\
&\quad \times \left[(r_2 r_3 (x_3 - x_2) - x_2) E_{an}(t_{an}^{(1c)}) a_i(t_{an}^{(1c)}) h_{an}^{(1c)}(x_i, b_i) \right. \\
&\quad \left. - (r_2 r_3 (x_2 - x_3) - x_3) E_{an}(t_{an}^{(2c)}) a_i(t_{an}^{(2c)}) h_{an}^{(2c)}(x_i, b_i) \right], \tag{C13}
\end{aligned}$$

$$\begin{aligned}
F_{anc}^{SP}(a_i(t)) &= 16\pi\sqrt{\frac{2}{3}}C_F m_B^4 \int_0^1 [dx] \int_0^{1/\Lambda} b_1 db_1 b_2 db_2 \phi_B(x_1, b_1) \phi_{M_2}(x_2) \phi_{M_3}(x_3) \\
&\quad \times \left[-(r_2 r_3 (x_2 - x_3) - x_3) E_{an}(t_{an}^{(1c)}) a_i(t_{an}^{(1c)}) h_{an}^{(1c)}(x_i, b_i) \right. \\
&\quad \left. ((-r_2 r_3 - 1)x_2 + r_2 r_3 x_3) E_{an}(t_{an}^{(2c)}) a_i(t_{an}^{(2c)}) h_{an}^{(2c)}(x_i, b_i) \right], \tag{C14}
\end{aligned}$$

Appendix D: factorization formulae for $B \rightarrow VV$

1. Longitudinal polarization

$$\begin{aligned}
F_e^{LL}(a_i(t)) &= 8\pi C_F f_{M_3} m_B^4 \int_0^1 dx_1 dx_2 \int_0^{1/\Lambda} b_1 db_1 b_2 db_2 \phi_B(x_1, b_1) \phi_{M_2}(x_2) \\
&\quad \times \left[(-1 - x_2 + r_2(2x_2 - 1)) E_e(t_e^{(1)}) a_i(t_e^{(1)}) h_e(x_1, x_2(1 - r_3^2), b_1, b_2) S_t(x_2) \right. \\
&\quad \left. - r_2(1 + r_2) E_e(t_e^{(2)}) a_i(t_e^{(2)}) h_e(x_2, x_1(1 - r_3^2), b_2, b_1) S_t(x_1) \right], \tag{D1}
\end{aligned}$$

$$F_e^{SP}(a_i(t)) = 0, \tag{D2}$$

$$\begin{aligned}
F_{en}^{LL}(a_i(t)) &= 16\pi\sqrt{\frac{2}{3}}C_F m_B^4 \int_0^1 [dx] \int_0^{1/\Lambda} b_1 db_1 b_3 db_3 \phi_B(x_1, b_1) \phi_{M_2}(x_2) \phi_{M_3}(x_3) \\
&\quad \times \left[(-x_2 r_2 - x_3) E_b(t_{en}^{(1)}) a_i(t_{en}^{(1)}) h_{en}^{(1)}(x_i, b_i) \right. \\
&\quad \left. - (x_2 r_2 - x_2 + x_3 - 1) E_{en}(t_{en}^{(2)}) a_i(t_{en}^{(2)}) h_{en}^{(2)}(x_i, b_i) \right], \tag{D3}
\end{aligned}$$

$$\begin{aligned}
F_{en}^{LR}(a_i(t)) &= 16\pi\sqrt{\frac{2}{3}}C_F m_B^4 \int_0^1 [dx] \int_0^{1/\Lambda} b_1 db_1 b_3 db_3 \phi_B(x_1, b_1) \phi_{M_2}(x_2) \phi_{M_3}(x_3) \\
&\quad \times r_3 \left[-(r_2(x_3 + x_2) - x_3) E_{en}(t_{en}^{(1)}) a_i(t_{en}^{(1)}) h_{en}^{(1)}(x_i, b_i) \right. \\
&\quad \left. - (x_3 + r_2(x_2 - x_3)) E_{en}(t_{en}^{(2)}) a_i(t_{en}^{(2)}) h_{en}^{(2)}(x_i, b_i) \right], \tag{D4}
\end{aligned}$$

$$\begin{aligned}
F_a^{LL}(a_i(t)) &= 8\pi C_F f_B m_B^4 \int_0^1 dx_2 dx_3 \int_0^{1/\Lambda} b_2 db_2 b_3 db_3 \phi_{M_2}(x_2) \phi_{M_3}(x_3) \\
&\quad \times \left[(-x_2 + 1) E_a(t_a^{(1)}) a_i(t_a^{(1)}) h_a(1 - (1 - r_2^2)x_3, 1 - (1 - r_3^2)x_2, b_3, b_2) S_t(x_2) \right. \\
&\quad \left. - (1 - x_3) E_a(t_a^{(2)}) a_i(t_a^{(2)}) h_a(1 - (1 - r_3^2)x_2, 1 - (1 - r_2^2)x_3, b_2, b_3) S_t(x_3) \right], \tag{D5}
\end{aligned}$$

$$F_a^{LR}(a_i(t)) = F_a^{LL}(a_i(t)), \tag{D6}$$

$$\begin{aligned}
F_a^{SP}(a_i(t)) &= 16\pi C_F f_B m_B^4 \int_0^1 dx_2 dx_3 \int_0^{1/\Lambda} b_2 db_2 b_3 db_3 \phi_{M_2}(x_2) \phi_{M_3}(x_3) \\
&\quad \times \left[r_2(x_2 - 1) E_a(t_a^{(1)}) a_i(t_a^{(1)}) h_a(1 - (1 - r_2^2)x_3, 1 - (1 - r_3^2)x_2, b_3, b_2) S_t(x_2) \right. \\
&\quad \left. + r_3(x_3 - 1) E_a(t_a^{(2)}) a_i(t_a^{(2)}) h_a(1 - (1 - r_3^2)x_2, 1 - (1 - r_2^2)x_3, b_2, b_3) S_t(x_3) \right], \tag{D7}
\end{aligned}$$

$$F_{ac}^{LL}(a_i(t)) = 0, \quad (D8)$$

$$F_{ac}^{LR}(a_i(t)) = F_{ac}^{LL}(a_i(t)) = 0, \quad (D9)$$

$$\begin{aligned} F_{an}^{LL}(a_i(t)) &= 16\pi\sqrt{\frac{2}{3}}C_F m_B^4 \int_0^1 [dx] \int_0^{1/\Lambda} b_1 db_1 b_2 db_2 \phi_B(x_1, b_1) \phi_{M_2}(x_2) \phi_{M_3}(x_3) \\ &\times \left[(-r_3 r_2 (x_2 + x_3) - x_3 + 1) E_{an}(t_{an}^{(1)}) a_i(t_{an}^{(1)}) h_{an}^{(1)}(x_i, b_i) \right. \\ &\left. - (-r_2 r_3 (x_2 + x_3 - 2) - x_2 + 1) E_{an}(t_{an}^{(2)}) a_i(t_{an}^{(2)}) h_{an}^{(2)}(x_i, b_i) \right], \end{aligned} \quad (D10)$$

$$\begin{aligned} F_{an}^{LR}(a_i(t)) &= 16\pi\sqrt{\frac{2}{3}}C_F m_B^4 \int_0^1 [dx] \int_0^{1/\Lambda} b_1 db_1 b_2 db_2 \phi_B(x_1, b_1) \phi_{M_2}(x_2) \phi_{M_3}(x_3) \\ &\times \left[-(-r_3(1 + x_3) + r_2(1 + x_2)) E_{an}(t_{an}^{(1)}) a_i(t_{an}^{(1)}) h_{an}^{(1)}(x_i, b_i) \right. \\ &\left. + (r_2(x_2 - 1) - r_3(x_3 - 1)) E_{an}(t_{an}^{(2)}) a_i(t_{an}^{(2)}) h_{an}^{(2)}(x_i, b_i) \right], \end{aligned} \quad (D11)$$

$$\begin{aligned} F_{an}^{SP}(a_i(t)) &= 16\pi\sqrt{\frac{2}{3}}C_F m_B^4 \int_0^1 [dx] \int_0^{1/\Lambda} b_1 db_1 b_2 db_2 \phi_B(x_1, b_1) \phi_{M_2}(x_2) \phi_{M_3}(x_3) \\ &\times \left[(-r_2 r_3 (x_2 + x_3) - x_2 + 1) E_{an}(t_{an}^{(1)}) a_i(t_{an}^{(1)}) h_{an}^{(1)}(x_i, b_i) \right. \\ &\left. - (-r_2 r_3 (x_2 + x_3 - 2) - (x_3 - 1)) E_{an}(t_{an}^{(2)}) a_i(t_{an}^{(2)}) h_{an}^{(2)}(x_i, b_i) \right], \end{aligned} \quad (D12)$$

$$\begin{aligned} F_{anc}^{LL}(a_i(t)) &= 16\pi\sqrt{\frac{2}{3}}C_F m_B^4 \int_0^1 [dx] \int_0^{1/\Lambda} b_1 db_1 b_2 db_2 \phi_B(x_1, b_1) \phi_{M_2}(x_2) \phi_{M_3}(x_3) \\ &\times \left[-(-r_2 r_3 (x_2 + x_3 - 2) - x_2) E_{an}(t_{an}^{(1c)}) a_i(t_{an}^{(1c)}) h_{an}^{(1c)}(x_i, b_i) \right. \\ &\left. + (-r_2 r_3 (x_2 + x_3) - x_3) E_{an}(t_{an}^{(2c)}) a_i(t_{an}^{(2c)}) h_{an}^{(2c)}(x_i, b_i) \right], \end{aligned} \quad (D13)$$

$$\begin{aligned} F_{anc}^{SP}(a_i(t)) &= 16\pi\sqrt{\frac{2}{3}}C_F m_B^4 \int_0^1 [dx] \int_0^{1/\Lambda} b_1 db_1 b_2 db_2 \phi_B(x_1, b_1) \phi_{M_2}(x_2) \phi_{M_3}(x_3) \\ &\times \left[-(-r_2 r_3 (x_2 + x_3 - 2) - x_3) E_{an}(t_{an}^{(1c)}) a_i(t_{an}^{(1c)}) h_{an}^{(1c)}(x_i, b_i) \right. \\ &\left. + ((-r_2 r_3 - 1)x_2 - r_3 r_2 x_3) E_{an}(t_{an}^{(2c)}) a_i(t_{an}^{(2c)}) h_{an}^{(2c)}(x_i, b_i) \right], \end{aligned} \quad (D14)$$

2. Transverse Polarization

$$\begin{aligned} F_e^{LL,s}(a_i(t)) &= 8\pi C_F f_{M_3} m_B^4 \int_0^1 dx_1 dx_2 \int_0^{1/\Lambda} b_1 db_1 b_2 db_2 \phi_B(x_1, b_1) \phi_{M_2}(x_2) \\ &\times r_3 \left[-(r_2(x_2 + 2) + 1) E_e(t_e^{(1)}) a_i(t_e^{(1)}) h_e(x_1, x_2(1 - r_3^2), b_1, b_2) S_t(x_2) \right. \\ &\left. - r_2 E_e(t_e^{(2)}) a_i(t_e^{(2)}) h_e(x_2, x_1(1 - r_3^2), b_2, b_1) S_t(x_1) \right], \end{aligned} \quad (D15)$$

$$\begin{aligned} F_e^{LL,p}(a_i(t)) &= 8\pi C_F f_{M_3} m_B^4 \int_0^1 dx_1 dx_2 \int_0^{1/\Lambda} b_1 db_1 b_2 db_2 \phi_B(x_1, b_1) \phi_{M_2}(x_2) \\ &\times r_3 \left[(r_2 x_2 - 1) E_e(t_e^{(1)}) a_i(t_e^{(1)}) h_e(x_1, x_2(1 - r_3^2), b_1, b_2) S_t(x_2) \right. \\ &\left. - r_2 E_e(t_e^{(2)}) a_i(t_e^{(2)}) h_e(x_2, x_1(1 - r_3^2), b_2, b_1) S_t(x_1) \right], \end{aligned} \quad (D16)$$

$$F_e^{SP,s}(a_i(t)) = F_e^{SP,p}(a_i(t)) = 0, \quad (D17)$$

$$\begin{aligned}
F_{en}^{LL,s}(a_i(t)) &= 16\pi\sqrt{\frac{2}{3}}C_F m_B^4 \int_0^1 [dx] \int_0^{1/\Lambda} b_1 db_1 b_3 db_3 \phi_B(x_1, b_1) \phi_{M_2}(x_2) \phi_{M_3}(x_3) \\
&\quad \times r_3 \left[-x_3 E_b(t_{en}^{(1)}) a_i(t_{en}^{(1)}) h_{en}^{(1)}(x_i, b_i) + (1 + x_3 + r_2(2x_2 - 2x_3 + 1)) E_{en}(t_{en}^{(2)}) a_i(t_{en}^{(2)}) h_{en}^{(2)}(x_i, b_i) \right] \quad (D18)
\end{aligned}$$

$$\begin{aligned}
F_{en}^{LL,p}(a_i(t)) &= 16\pi\sqrt{\frac{2}{3}}C_F m_B^4 \int_0^1 [dx] \int_0^{1/\Lambda} b_1 db_1 b_3 db_3 \phi_B(x_1, b_1) \phi_{M_2}(x_2) \phi_{M_3}(x_3) \\
&\quad \times r_3 \left[-x_3 E_b(t_{en}^{(1)}) a_i(t_{en}^{(1)}) h_{en}^{(1)}(x_i, b_i) + (1 + x_3 - r_2) E_{en}(t_{en}^{(2)}) a_i(t_{en}^{(2)}) h_{en}^{(2)}(x_i, b_i) \right], \quad (D19)
\end{aligned}$$

$$\begin{aligned}
F_{en}^{LR,s}(a_i(t)) &= 16\pi\sqrt{\frac{2}{3}}C_F m_B^4 \int_0^1 [dx] \int_0^{1/\Lambda} b_1 db_1 b_3 db_3 \phi_B(x_1, b_1) \phi_{M_2}(x_2) \phi_{M_3}(x_3) \\
&\quad \times \left[-(x_2 r_2^2 - x_2 r_2 + r_3^2 x_3) E_{en}(t_{en}^{(1)}) a_i(t_{en}^{(1)}) h_{en}^{(1)}(x_i, b_i) \right. \\
&\quad \left. - (x_2 r_2^2 - x_2 r_2 - r_3^2 x_3) E_{en}(t_{en}^{(2)}) a_i(t_{en}^{(2)}) h_{en}^{(2)}(x_i, b_i) \right], \quad (D20)
\end{aligned}$$

$$\begin{aligned}
F_{en}^{LR,p}(a_i(t)) &= 16\pi\sqrt{\frac{2}{3}}C_F m_B^4 \int_0^1 [dx] \int_0^{1/\Lambda} b_1 db_1 b_3 db_3 \phi_B(x_1, b_1) \phi_{M_2}(x_2) \phi_{M_3}(x_3) \\
&\quad \times \left[-(x_2 r_2^2 - x_2 r_2 - r_3^2 x_3) E_{en}(t_{en}^{(1)}) a_i(t_{en}^{(1)}) h_{en}^{(1)}(x_i, b_i) \right. \\
&\quad \left. - (x_2 r_2^2 - x_2 r_2 + r_3^2 x_3) E_{en}(t_{en}^{(2)}) a_i(t_{en}^{(2)}) h_{en}^{(2)}(x_i, b_i) \right], \quad (D21)
\end{aligned}$$

$$\begin{aligned}
F_a^{LL,s}(a_i(t)) &= 8\pi C_F f_B m_B^4 \int_0^1 dx_2 dx_3 \int_0^{1/\Lambda} b_2 db_2 b_3 db_3 \phi_{M_2}(x_2) \phi_{M_3}(x_3) \\
&\quad \times r_2 r_3 \left[(2 - x_2) E_a(t_a^{(1)}) a_i(t_a^{(1)}) h_a(1 - (1 - r_2^2)x_3, 1 - (1 - r_3^2)x_2, b_3, b_2) S_t(x_2) \right. \\
&\quad \left. + (x_3 - 2) E_a(t_a^{(2)}) a_i(t_a^{(2)}) h_a(1 - (1 - r_3^2)x_2, 1 - (1 - r_2^2)x_3, b_2, b_3) S_t(x_3) \right], \quad (D22)
\end{aligned}$$

$$\begin{aligned}
F_a^{LL,p}(a_i(t)) &= 8\pi C_F f_B m_B^4 \int_0^1 dx_2 dx_3 \int_0^{1/\Lambda} b_2 db_2 b_3 db_3 \phi_{M_2}(x_2) \phi_{M_3}(x_3) \\
&\quad \times r_2 r_3 \left[x_2 E_a(t_a^{(1)}) a_i(t_a^{(1)}) h_a(1 - (1 - r_2^2)x_3, 1 - (1 - r_3^2)x_2, b_3, b_2) S_t(x_2) \right. \\
&\quad \left. + x_3 E_a(t_a^{(2)}) a_i(t_a^{(2)}) h_a(1 - (1 - r_3^2)x_2, 1 - (1 - r_2^2)x_3, b_2, b_3) S_t(x_3) \right], \quad (D23)
\end{aligned}$$

$$F_a^{LR,s}(a_i(t)) = F_a^{LL,s}(a_i(t)), \quad (D24)$$

$$F_a^{LR,p}(a_i(t)) = -F_a^{LL,p}(a_i(t)), \quad (D25)$$

$$\begin{aligned}
F_a^{SP,s}(a_i(t)) &= 16\pi C_F f_B m_B^4 \int_0^1 dx_2 dx_3 \int_0^{1/\Lambda} b_2 db_2 b_3 db_3 \phi_{M_2}(x_2) \phi_{M_3}(x_3) \\
&\quad \times \left[-r_3 E_a(t_a^{(1)}) a_i(t_a^{(1)}) h_a(1 - (1 - r_2^2)x_3, 1 - (1 - r_3^2)x_2, b_3, b_2) S_t(x_2) \right. \\
&\quad \left. - r_2 E_a(t_a^{(2)}) a_i(t_a^{(2)}) h_a(1 - (1 - r_3^2)x_2, 1 - (1 - r_2^2)x_3, b_2, b_3) S_t(x_3) \right], \quad (D26)
\end{aligned}$$

$$F_a^{SP,p}(a_i(t)) = F_a^{SP,s}(a_i(t)), \quad (D27)$$

$$\begin{aligned}
F_{ac}^{LL,s}(a_i(t)) &= 8\pi C_F f_B m_B^4 \int_0^1 dx_2 dx_3 \int_0^{1/\Lambda} b_2 db_2 b_3 db_3 \phi_{M_2}(x_2) \phi_{M_3}(x_3) \\
&\quad \times \left[-r_2 (r_2 - r_3(x_3 + 1)) E_a(t_a^{(1c)}) a_i(t_a^{(1c)}) h_a(x_2, x_3(1 - r_2^2 - r_3^2), b_2, b_3) S_t(x_3) \right. \\
&\quad \left. + r_3 (r_3 - r_2(x_2 + 1)) E_a(t_a^{(2c)}) a_i(t_a^{(2c)}) h_a(x_3, x_2(1 - r_2^2 - r_3^2), b_3, b_2) S_t(x_2) \right], \quad (D28)
\end{aligned}$$

$$\begin{aligned}
F_{ac}^{LL,p}(a_i(t)) &= 8\pi C_F f_B m_B^4 \int_0^1 dx_2 dx_3 \int_0^{1/\Lambda} b_2 db_2 b_3 db_3 \phi_{M_2}(x_2) \phi_{M_3}(x_3) \\
&\times \left[r_2(r_2 - r_3(x_3 - 1)) E_a(t_a^{(1c)}) a_i(t_a^{(1c)}) h_a(x_2, x_3(1 - r_2^2 - r_3^2), b_2, b_3) S_t(x_3) \right. \\
&\left. + r_3(r_3 - r_2(x_2 - 1)) E_a(t_a^{(2c)}) a_i(t_a^{(2c)}) h_a(x_3, x_2(1 - r_2^2 - r_3^2), b_3, b_2) S_t(x_2) \right], \tag{D29}
\end{aligned}$$

$$F_{ac}^{LR,s}(a_i(t)) = F_{ac}^{LL,s}(a_i(t)), \tag{D30}$$

$$F_{ac}^{LR,p}(a_i(t)) = -F_{ac}^{LL,p}(a_i(t)), \tag{D31}$$

$$\begin{aligned}
F_{an}^{LL,s}(a_i(t)) &= 16\pi \sqrt{\frac{2}{3}} C_F m_B^4 \int_0^1 [dx] \int_0^{1/\Lambda} b_1 db_1 b_2 db_2 \phi_B(x_1, b_1) \phi_{M_2}(x_2) \phi_{M_3}(x_3) \\
&\times \left[-(x_2 r_2^2 - 2r_2 r_3 + r_3^2 x_3) E_{an}(t_{an}^{(1)}) a_i(t_{an}^{(1)}) h_{an}^{(1)}(x_i, b_i) \right. \\
&\left. + ((x_2 - 1)r_2^2 + r_3^2(x_3 - 1)) E_{an}(t_{an}^{(2)}) a_i(t_{an}^{(2)}) h_{an}^{(2)}(x_i, b_i) \right], \tag{D32}
\end{aligned}$$

$$\begin{aligned}
F_{an}^{LL,p}(a_i(t)) &= 16\pi \sqrt{\frac{2}{3}} C_F m_B^4 \int_0^1 [dx] \int_0^{1/\Lambda} b_1 db_1 b_2 db_2 \phi_B(x_1, b_1) \phi_{M_2}(x_2) \phi_{M_3}(x_3) \\
&\times \left[(r_3^2 x_3 - r_2^2 x_2) E_{an}(t_{an}^{(1)}) a_i(t_{an}^{(1)}) h_{an}^{(1)}(x_i, b_i) \right. \\
&\left. + (r_2^2(x_2 - 1) - r_3^2(x_3 - 1)) E_{an}(t_{an}^{(2)}) a_i(t_{an}^{(2)}) h_{an}^{(2)}(x_i, b_i) \right], \tag{D33}
\end{aligned}$$

$$\begin{aligned}
F_{an}^{LR,s}(a_i(t)) &= 16\pi \sqrt{\frac{2}{3}} C_F m_B^4 \int_0^1 [dx] \int_0^{1/\Lambda} b_1 db_1 b_2 db_2 \phi_B(x_1, b_1) \phi_{M_2}(x_2) \phi_{M_3}(x_3) \\
&\times \left[(r_2(x_2 + 1) - r_3(x_3 + 1)) E_{an}(t_{an}^{(1)}) a_i(t_{an}^{(1)}) h_{an}^{(1)}(x_i, b_i) \right. \\
&\left. - (r_2(x_2 - 1) - r_3(x_3 - 1)) E_{an}(t_{an}^{(2)}) a_i(t_{an}^{(2)}) h_{an}^{(2)}(x_i, b_i) \right], \tag{D34}
\end{aligned}$$

$$F_{an}^{LR,p}(a_i(t)) = F_{an}^{LR,s}(a_i(t)), \tag{D35}$$

$$\begin{aligned}
F_{an}^{SP,s}(a_i(t)) &= 16\pi \sqrt{\frac{2}{3}} C_F m_B^4 \int_0^1 [dx] \int_0^{1/\Lambda} b_1 db_1 b_2 db_2 \phi_B(x_1, b_1) \phi_{M_2}(x_2) \phi_{M_3}(x_3) \\
&\times \left[-(x_2 r_2^2 - 2r_2 r_3 + r_3^2 x_3) E_{an}(t_{an}^{(1)}) a_i(t_{an}^{(1)}) h_{an}^{(1)}(x_i, b_i) \right. \\
&\left. + ((x_2 - 1)r_2^2 + r_3^2(x_3 - 1)) E_{an}(t_{an}^{(2)}) a_i(t_{an}^{(2)}) h_{an}^{(2)}(x_i, b_i) \right], \tag{D36}
\end{aligned}$$

$$\begin{aligned}
F_{an}^{SP,p}(a_i(t)) &= 16\pi \sqrt{\frac{2}{3}} C_F m_B^4 \int_0^1 [dx] \int_0^{1/\Lambda} b_1 db_1 b_2 db_2 \phi_B(x_1, b_1) \phi_{M_2}(x_2) \phi_{M_3}(x_3) \\
&\times \left[(r_2^2 x_2 - r_3^2 x_3) E_{an}(t_{an}^{(1)}) a_i(t_{an}^{(1)}) h_{an}^{(1)}(x_i, b_i) \right. \\
&\left. - (r_2^2(x_2 - 1) - r_3^2(x_3 - 1)) E_{an}(t_{an}^{(2)}) a_i(t_{an}^{(2)}) h_{an}^{(2)}(x_i, b_i) \right], \tag{D37}
\end{aligned}$$

$$\begin{aligned}
F_{anc}^{LL,s}(a_i(t)) &= 16\pi \sqrt{\frac{2}{3}} C_F m_B^4 \int_0^1 [dx] \int_0^{1/\Lambda} b_1 db_1 b_2 db_2 \phi_B(x_1, b_1) \phi_{M_2}(x_2) \phi_{M_3}(x_3) \\
&\times \left[((x_2 - 1)r_2^2 + 2r_2 r_3 + r_3^2(x_3 - 1)) E_{an}(t_{an}^{(1c)}) a_i(t_{an}^{(1c)}) h_{an}^{(1c)}(x_i, b_i) \right. \\
&\left. - (x_2 r_2^2 + x_3 r_3^2) E_{an}(t_{an}^{(2c)}) a_i(t_{an}^{(2c)}) h_{an}^{(2c)}(x_i, b_i) \right], \tag{D38}
\end{aligned}$$

$$\begin{aligned}
F_{anc}^{LL,p}(a_i(t)) &= 16\pi\sqrt{\frac{2}{3}}C_F m_B^4 \int_0^1 [dx] \int_0^{1/\Lambda} b_1 db_1 b_2 db_2 \phi_B(x_1, b_1) \phi_{M_2}(x_2) \phi_{M_3}(x_3) \\
&\times \left[- (r_2^2(x_2 - 1) - r_3^2(x_3 - 1)) E_{an}(t_{an}^{(1c)}) a_i(t_{an}^{(1c)}) h_{an}^{(1c)}(x_i, b_i) \right. \\
&\left. + (x_2 r_2^2 - x_3 r_3^2) E_{an}(t_{an}^{(2c)}) a_i(t_{an}^{(2c)}) h_{an}^{(2c)}(x_i, b_i) \right], \tag{D39}
\end{aligned}$$

$$\begin{aligned}
F_{anc}^{SP,s}(a_i(t)) &= 16\pi\sqrt{\frac{2}{3}}C_F m_B^4 \int_0^1 [dx] \int_0^{1/\Lambda} b_1 db_1 b_2 db_2 \phi_B(x_1, b_1) \phi_{M_2}(x_2) \phi_{M_3}(x_3) \\
&\times \left[((x_2 - 1)r_2^2 + 2r_2 r_3 + r_3^2(x_3 - 1)) E_{an}(t_{an}^{(1c)}) a_i(t_{an}^{(1c)}) h_{an}^{(1c)}(x_i, b_i) \right. \\
&\left. + (r_2^2(x_2 - 1) - r_3^2(x_3 - 1)) E_{an}(t_{an}^{(2c)}) a_i(t_{an}^{(2c)}) h_{an}^{(2c)}(x_i, b_i) \right], \tag{D40}
\end{aligned}$$

$$\begin{aligned}
F_{anc}^{SP,p}(a_i(t)) &= 16\pi\sqrt{\frac{2}{3}}C_F m_B^4 \int_0^1 [dx] \int_0^{1/\Lambda} b_1 db_1 b_2 db_2 \phi_B(x_1, b_1) \phi_{M_2}(x_2) \phi_{M_3}(x_3) \\
&\times \left[(r_2^2(x_2 - 1) - r_3^2(x_3 - 1)) E_{an}(t_{an}^{(1c)}) a_i(t_{an}^{(1c)}) h_{an}^{(1c)}(x_i, b_i) \right. \\
&\left. - (r_2^2 x_2 - r_3^2 x_3) E_{an}(t_{an}^{(2c)}) a_i(t_{an}^{(2c)}) h_{an}^{(2c)}(x_i, b_i) \right], \tag{D41}
\end{aligned}$$

-
- [1] Y.Y. Keum, et al., Phys. Rev. D69, 094018 (2004), e-Print: hep-ph/0305335; C.-D. Lu, Phys. Rev. D68, 097502 (2003), e-Print: hep-ph/0307040; G.L. Song, C.-D. Lu, Phys. Rev. D70, 034006 (2004), e-Print: hep-ph/0403233; J.-F. Cheng, D.-S. Du, C.-D. Lu, Eur. Phys. J. C45, 711 (2006), e-Print: hep-ph/0501082
- [2] S. Fratina *et al.*, Phys. Rev. Lett. **98**, 221802 (2007) [arXiv:hep-ex/0702031].
- [3] B. Aubert *et al.* [BaBar Collaboration], Phys. Rev. Lett. **99**, 071801 (2007) [arXiv:0705.1190 [hep-ex]].
- [4] B. Aubert *et al.* [BaBar Collaboration], Phys. Rev. D **76**, 111102 (2007) [arXiv:0708.1549 [hep-ex]].
I. Adachi *et al.* [Belle Collaboration], Phys. Rev. D **77**, 091101 (2008) [arXiv:0802.2988 [hep-ex]].
H. Miyake *et al.* [Belle Collaboration], Phys. Lett. B **618**, 34 (2005) [arXiv:hep-ex/0501037].
T. Aushev *et al.* [BELLE Collaboration], Phys. Rev. Lett. **93**, 201802 (2004) [arXiv:hep-ex/0408051].
- [5] R. Fleischer, Eur. Phys. J. C **51**, 849 (2007) [arXiv:0705.4421 [hep-ph]].
- [6] M. Gronau, J. L. Rosner and D. Pirjol, Phys. Rev. D **78**, 033011 (2008) [arXiv:0805.4601 [hep-ph]].
- [7] C. S. Kim, R. M. Wang and Y. D. Yang, arXiv:0812.4136 [hep-ph].
- [8] Y. Li, C.D. Lu, J. Phys. G31, 273 (2005), e-Print: hep-ph/0308243.
- [9] Y.-Y. Keum, H.-n. Li and A. I. Sanda, Phys. Lett. B504, 6 (2001); Phys. Rev. D63, 054008 (2001); C.-D. Lü, K. Ukai and M.-Z. Yang, Phys. Rev. D63, 074009 (2001); C.-D. Lü and M.-Z. Yang, Eur. Phys. J. C23, 275-287 (2002).
- [10] B. H. Hong and C. D. Lu, Sci. China G **49**, 357 (2006) [arXiv:hep-ph/0505020].
- [11] C.D. Lu, K. Ukai, Eur. Phys. J. C28, 305 (2003), e-Print: hep-ph/0210206; Y. Li, C.D. Lu, J. Phys. G29, 2115 (2003), e-Print: hep-ph/0304288; High Energy Phys. & Nucl. Phys. 27, 1062 (2003), e-Print: hep-ph/0305278.
- [12] C.W.Bauer, D. Pirjol, I.W.Stewart, Phys. Rev. Lett. 87(2001) 201806 [hep-ph/0107002]; Phys. Rev. D65,054022 (2002) [hep-ph/0109045].
- [13] R. H. Li, C. D. Lu and H. Zou, Phys. Rev. D **78**, 014018 (2008) [arXiv:0803.1073 [hep-ph]].
- [14] For a review, see G. Buchalla, A. J. Buras and M. E. Lautenbacher, Rev. Mod. Phys. **68**, 1125 (1996) [arXiv:hep-ph/9512380].

- [15] A. Ali, G. Kramer and C. D. Lu, Phys. Rev. D **58**, 094009 (1998) [arXiv:hep-ph/9804363].
- [16] C. D. Lu and M. Z. Yang, Eur. Phys. J. C **28**, 515 (2003) [arXiv:hep-ph/0212373].
- [17] T. Kurimoto, H. n. Li and A. I. Sanda, Phys. Rev. D **67**, 054028 (2003) [arXiv:hep-ph/0210289].
- [18] C. Amsler et al. (Particle Data Group), Physics Letters B667, 1 (2008).
- [19] A. J. Buras, arXiv:hep-ph/9806471; I.I. Y. Bigi and A.I. Sanda, *CP Violation*, Cambridge Monogr., Part. Phys. Nucl. Phys. Cosmol. **9**, 1(2000); G.C. Branco, L. Lavoura, and J.P. Silva, *CP Violation*, Oxford University Press, Oxford (1999).
- [20] These values are from the website of CKM fitter group: <http://ckmfitter.in2p3.fr/>.
- [21] E. Follana, C. T. H. Davies, G. P. Lepage and J. Shigemitsu [HPQCD Collaboration and UKQCD Collaboration], Phys. Rev. Lett. **100**, 062002 (2008) [arXiv:0706.1726 [hep-lat]].
- [22] A. V. Manohar and M. B. Wise, Camb. Monogr. Part. Phys. Nucl. Phys. Cosmol. **10**, 1 (2000).
- [23] A. Zupanc *et al.*, Phys. Rev. D **75**, 091102 (2007) [arXiv:hep-ex/0703040].
- [24] B. Aubert *et al.* [BABAR Collaboration], Phys. Rev. D **72**, 111101 (2005) [arXiv:hep-ex/0510051].
- [25] B. Aubert *et al.* [BABAR Collaboration], Phys. Rev. D **73**, 112004 (2006) [arXiv:hep-ex/0604037].
- [26] C. E. Thomas, Phys. Rev. D **73**, 054016 (2006) [arXiv:hep-ph/0511169].
- [27] C. H. Chen, C. Q. Geng and Z. T. Wei, Eur. Phys. J. C **46**, 367 (2006) [arXiv:hep-ph/0507295].
- [28] A. Ali, et al., Phys. Rev. D **76**, 074018 (2007) e-Print: hep-ph/0703162.
- [29] R. H. Li, C. D. Lu and Y. M. Wang, Phys. Rev. D **80**, 014005 (2009).
- [30] H. n. Li and S. Mishima, Phys. Rev. D **71**, 054025 (2005) [arXiv:hep-ph/0411146].